

## Response to Reviewers

We thank the reviewers for their comments. We have worked to address all concerns as discussed below, with a number of changes made to the manuscript and SI. We believe such changes increase the robustness of the conclusions, and generally have led to an improved manuscript.

Responses to specific comments are below. The original reviewer comment is in italics with the author response in normal font.

### Reviewer 1

#### Major Comments

*This work by Hagan and Kroll presents an open source model, opcsim, based on mie theory that they suggest can be used to evaluate the ability of low-cost optical particle sensors (optical particle counters and nephelometers) to accurately characterize the size distribution and/or mass loading of aerosol particles. The authors use this model to evaluate the ability of different sensor technology to measure PM<sub>2.5</sub> mass concentration and the effect of RH, aerosol composition and size distribution on these sensors. My concerns relate more to the authors use of the model to evaluate low cost-sensors and their conclusions from it. I realise that the authors did not want to be too specific (e.g. focusing on one particular sensor), but I did find that the findings are quite broad. I think this is best highlighted by their conclusion that the lower particle size cut off is critical, especially for low-cost particle sensors, as this can be relatively high (ca. 500nm). To me this is kind of obvious, even the very best OPC will not be able measure particles below their lower size bin. Consequently, it not surprising that this is a large source of error for a low cost OPC relative to an OPC that has a lower size cut off. In my opinion, the results from the model simulation seemed to be overly affected by the lower size cut off chosen for the low and high cost OPC*

As the reviewer mentions, we were intentionally broad, not showing results for a specific sensor model. This is by design, as there are simply too many specific sensors to complete an analysis for each individual one. This is why this model is open-sourced, with extensive documentation, is so that anyone can run the analysis for a specific sensor model. There is documentation with the model code (<https://github.com/dhhagan/opcsim>) showing how to do this for the Alphasense OPC-N2 – a generally available low-cost optical particle counter. In addition, we agree that “the very best OPC will not be able to measure particles below their lower size bin”. However, as a survey of the low-cost sensor literature will show, (1) this is not generally appreciated amongst this community; and (2) it has not been shown just how much of an impact this can have when making PM measurements using these devices across a wide range of environments and environmental conditions.

In order to clarify the objectives of this work, and specifically to explain why individual sensors are not systematically investigated, we have added the following text to the introduction:

The following text has been appended to the introduction:

The objective of this work is to describe the model and software and to investigate broad influences on aerosol properties and sensor parameters on measurement performance. This present work does not investigate the performance of individual commercially available sensors under the full range of conditions expected in the atmosphere; but such studies are enabled by this modeling tool and are an important future extension of this work.

*Overall, in my opinion, the paper is well written, clearly presented and the model will be of interest and use to the community to evaluate new sensors and their potential errors prior to lab testing.*

We thank the reviewer for their assessment and address the individual comments below.

### Minor Comments

*Page 20, line 19: The authors state 'Even under conditions where the aerosol is not absorbing, the low-cost OPC largely underestimates the mass due to its high minimum size cutoff' If the errors are associated more with the size cut off, then how can you make statements about the effect of aerosol refractive index on the low-cost sensor*

We are able to make these comments because we perform two separate experiments: (1) we hold the aerosol optical properties constant and change only the size distribution (Section 3.3); (2) we hold the size distribution constant and change only the aerosol optical properties (Section 3.2). This allows us to separate out the impact of each factor individually.

*Page 22, line 5: Is this issue with this comparison that the chosen model aerosol mostly falls below the size detection limit of the low cost OPC (is 500nm)? For me, when I look at Fig 5, when the GM of the aerosol is above 500nm the low cost OPC performs well. I do not quite see the point of this simulation, as these uncertainties related to lower size cut off are inherent for any OPC, irrespective if they are low or high cost?*

The reviewer is correct that these issues are inherent for any OPC irrespective of cost. However, the purpose of this figure is to demonstrate the relative ability of different OPSs to accurately measure varying size distributions. Yes, an OPC will do a good job for an aerosol distribution with a number-weighted GM ~ 500nm; however, there are very few instances where you might encounter a distribution that large in the real-world. Figure 5 shows that as the size cutoff of the OPC improves, the ability of the OPC to more

accurately size and count particles improves for a wider range of size distributions. Importantly, it also demonstrates that a nephelometer cannot adapt to changes in size distribution well at all, which is important because many low-cost, widely used AQ networks are based on the Plantower PMS5003 sensor, which is a nephelometer.

*Page 23. Line 8-10: Could you provide an estimation of the absolute error for low particle mass concentrations from the literature?*

It is difficult to report estimates for the absolute error as it depends largely on the exact area that data was collected and can be heavily influenced by the normalization of the size distribution via longer averaging times. The estimate for the error can be computed if the size distribution is known. A statement has been added to the conclusion that summarizes the need for improved co-location data with size-resolved measurements so that these numbers can be better understood: "Additionally, co-located data with size-resolved measurements would allow for improved validation of the OPC component of this model." (P 27, lines 6-8)

*Table 4: These NIST standards are very expensive, perhaps you could suggest cheaper alternatives?*

We have changed this column to include collected samples; these would be less standardized and less well-characterized, but also are substantially less expensive than the NIST standards listed.

## Reviewer 2

### Major Comments

*Low-cost sensors (LCSs) are widely used now-a-days for objectives ranging from citizen awareness to scientific research. Many studies have been conducted to evaluate commercially-available LCSs (including by my group), but systematic design-based analyses have been lacking. The recent He et al. (2019) <https://doi.org/10.1080/02786826.2019.1696015> and this submission are important steps towards overcoming that shortcoming. Some specific comments are listed below, but a broad comment is that the results as presented could be made more useful with simulations that consider widely-used commercial devices.*

Thank you for these comments. We completely agree that more device-specific comparisons would be very useful! First, however, we felt it was important to first (1) describe the approach used, (2) make the modeling tools available, and (3) investigate general considerations (related to aerosol properties and sensor parameters) related to measurement accuracy. In particular, we aimed to show that the size range for which the device can measure is very important as opposed to comparing specific instruments. We do have follow-up work planned that both compares the results of this model to field and

laboratory measurements by specific nephelometers and OPCs; but our hope is that this tool may also be useful to others to investigate sensor performance for specific sensors and/or aerosol types.

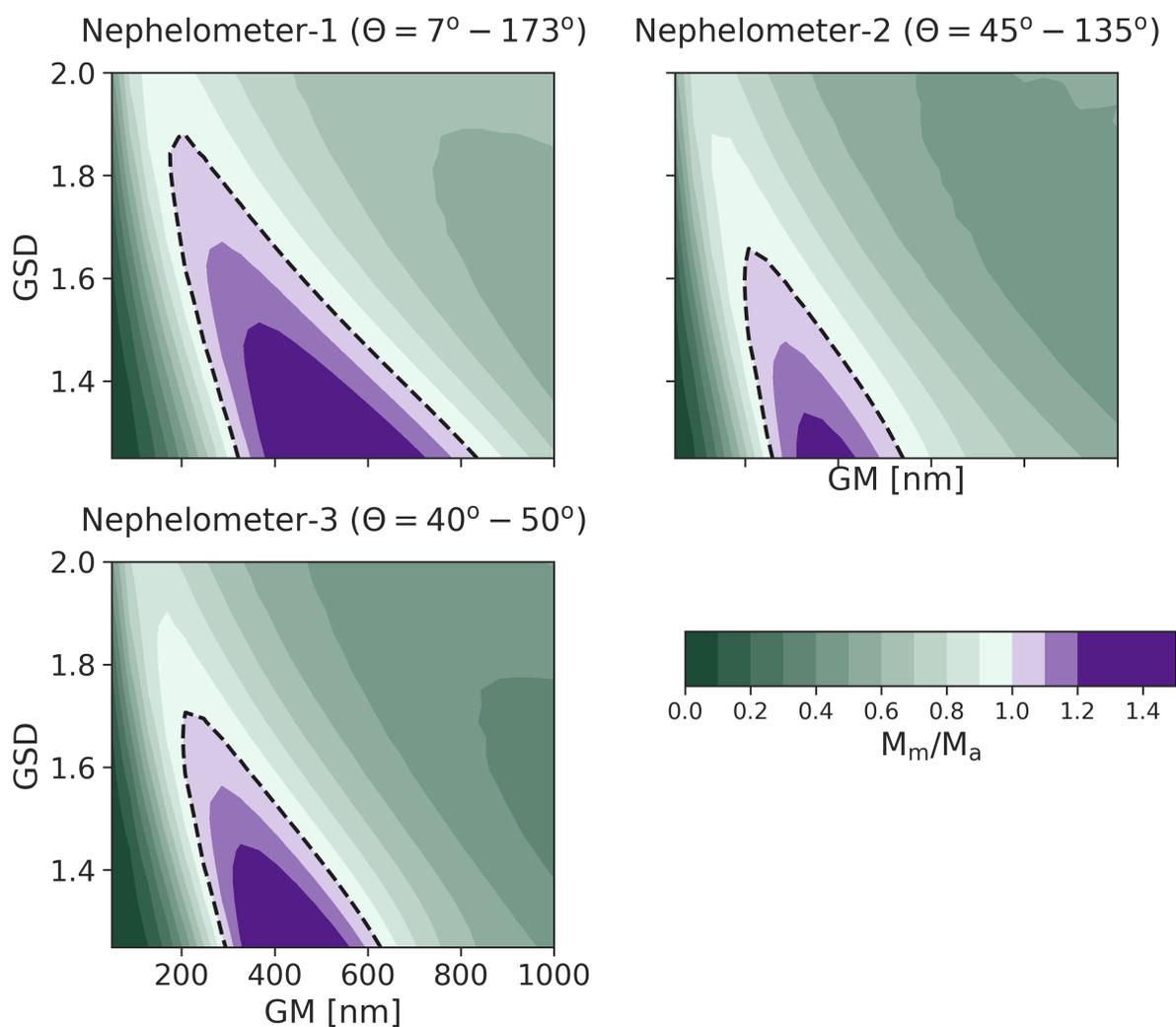
*For example, common high-end OPSs (TSI 640, Grimm 180) do not measure down to 100 nm, but rather to 180-200 nm. (The Handix POPS - a really nice instrument! I want one! - is not commonly used for ambient PM measurements and probably gets overwhelmed by ambient PN outside of balloon flights.) I suspect this higher cutoff will significantly worsen the performance of the high-end OPC presented here, but it will be more realistic.*

This is a very good point and comes down to the definition of 'high-end' – whether it's the best one possible or the best one widely available/used. We chose the former, as a rough estimate of the smallest particle size that an optical sensor could reasonably measure. To make this clear, we now discuss this in the text: "We note that many expensive OPCs cannot measure particles down to 100 nm; this lower size cutoff was chosen as an approximate smallest particle size that an optical sensor can detect." (P 14, lines 11-12)

*The nephelometer collection angle used here is 7-173 degrees, which may be true for expensive TSI-type nephelometers, but such data are not available for LCSs (as shown in Table 1). The best data might be from Kelly et al. (2017) <http://dx.doi.org/10.1016/j.envpol.2016.12.039>, who say the Plantower collects scattered light at 90 degrees and the Shinyei at 45 degrees. It might help if the nephelometer results presented in this manuscript instead used 90+/-45 degrees or a similar range (or maybe the Plantower company can provide that information?)*

As the reviewer points out, we did not systematically investigate the effect of viewing angle, which can vary from sensor to sensor. We agree that the center of the collection angle is at 90° for the Plantower, though from a physical inspection it does appear there is no real focusing of the collected light. The Shinyei would likely be classified as a photometer, which is considered a subset of the nephelometer in this work.

We have computed results for two alternate optical setups, one with a collection angle of 90 +/- 45 degrees, and another with a collection angle of 45 +/- 5 degrees. These results are shown below. While the range for which a 1:1 value is obtained do change with collection angle (as expected), the results are qualitatively the same. A section on this has been added to the SI, along with a new Figure S4 (shown below); this is referred to in the main text as well (P22 lines 3-5).



Finally, a key difference between the results presented here and sensor performance in the real world is that manufacturers may calibrate the sensor to ambient urban aerosol. This appears to be the case for Plantower - we were told (Malings et al. 2019) they calibrate to reference monitors in Chinese cities. (Met-One NPM is calibrated with 600 nm PSL.) Would it be possible to use a "typical" Beijing PSD instead of the ammonium sulfate calibration basis in the nephelometer results presented here?

We chose polydisperse ammonium sulfate as a standard for comparison across all nephelometer types. A Plantower-specific study should definitely include Beijing urban aerosol as the calibrant. We are currently working on applying opcsim to the Plantower, but as noted above, focusing on specific sensors is beyond the scope of this work.

*I admit some of this may be more complicated and a lot more work, but people wanting to use the opcsim software may invariably want to do just that... And might turn to Dr Hagan for assistance anyway! Might as well get ahead of the curve and also get it published.*

We agree and are working on specific use-cases; but we also didn't want to wait until that work was completed to describe (and release) the model. The number of specific sensors, aerosol types, and environmental conditions is too large to cover in a single study; so instead, we hope this can be useful to others to examine specific use cases. Each reader/user may want to simulate their sensor in a slightly different way with different calibrants and/or sensor specifications. To make this easier, extensive documentation showing exactly how to do this using this model can be found in the code's documentation (<https://dhhagan.github.io/opcsim/>). Questions pertaining to the code itself or to specific examples can be posted publicly on the GitHub repository itself (<https://github.com/dhhagan/opcsim>).

## Minor Comments

*Page 15, line 8: what is "actual PM2.5 mass"? Is that the mass at 35% RH (like EPA regulations)? Please specify.*

This paper calculates 'actual' mass at 0% RH. The difference between mass at 0% and 35% RH is negligible for most aerosols. Per Figure 2, with the exception of marine aerosol, kappa values are 0.25 or less. At a kappa of 0.25, the expected difference in mass at 35% relative to 0% RH is ~10%. This has been clarified in the text. (P 15, lines 8-9)

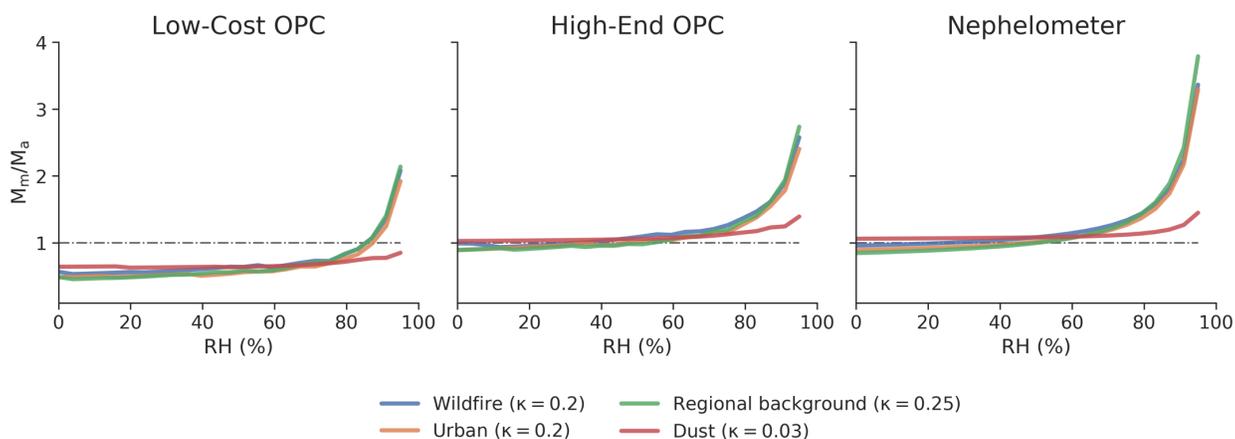
*Page 16, lines 18-20: wouldn't the "missing mass" problem be present at all humidities, just (over)compensated at higher RH due to hygroscopic growth?*

Yes, the reviewer is correct. The missing mass problem is present at all humidities and is simply over-compensated at higher RH. The text has been updated (P 16 lines 17-19) to make this clearer: "In addition to overestimating mass loadings at high relative humidity due to hygroscopic growth, the OPCs underestimate the mass loadings across all relative humidities. This is not caused by relative humidity or a lack of hygroscopic growth, but instead is a result of the "missing mass" below the detectable threshold of the OPC."

*Figure 2: Some of these results are hard to decipher on a log scale. Maybe show it on a linear scale? (The marine case seems to be an extreme/can be moved to SI?)*

We considered this, for the exact reasons the reviewer states. However, the linear scale actually makes the data harder to interpret, as the values for different aerosol types appear closer together. The linear-scale image (without marine) is shown below for reference.

Thus, we prefer to keep the figure with a log axis, to highlight differences between different particle types.



Also in Fig 2, at least in Malings et al. (2019), we showed errors in the as-reported Plantower data as a function of RH (Table S2). Perhaps a more RH-resolved comparison could be made?

This was the primary objective of Figure 2 (which is expressed as relative error rather than absolute error). However, these are calculations on model aerosol and not measurements of real-world particles (as in Malings 2020), so we prefer not to tabulate results, which might give the wrong impression about the applicability of these errors to real-world systems/sensors.

Page 18, lines 4-6: Can RI changes really cause such significant mis-assignment? Maybe at the margins/bin boundaries, sure. But the PSL, SOA, ammonium sulfate Mie curves (Fig 3) are pretty close to each other, and these are the dominant PM2.5 components by mass and (probably, OPC-wise anyway) number.

This is an important point, which we did not address explicitly in the original submission. We have added an additional section and multiple figures to the SI that shows just how much of an impact slight changes in RI can have on the bin assignment for an OPC. This new section in the SI shows that yes, even small changes in RI can lead to large changes in how a particle is assigned to a bin – it can span many bins for a given particle size and depends strongly on the properties of the OPC as well as the aerosol itself. These text and figures are given below:

### Impact of changes in aerosol optical properties on OPC bin assignment

Here we investigate how bin assignment may be affected if the aerosol optical properties of the measured aerosol are different than the material used to calibrate an OPC. We compute the light scattering for a range of possible refractive index values and plot them

in Figure S2 below for a 600 nm particle. Across a wide range of optical properties, the particle can be placed in 3 different bins or left out completely (“NO BIN”). However, it should be noted that fairly large changes in either the real or imaginary part of the RI need to change in order for a particle to be assigned to a different bin.

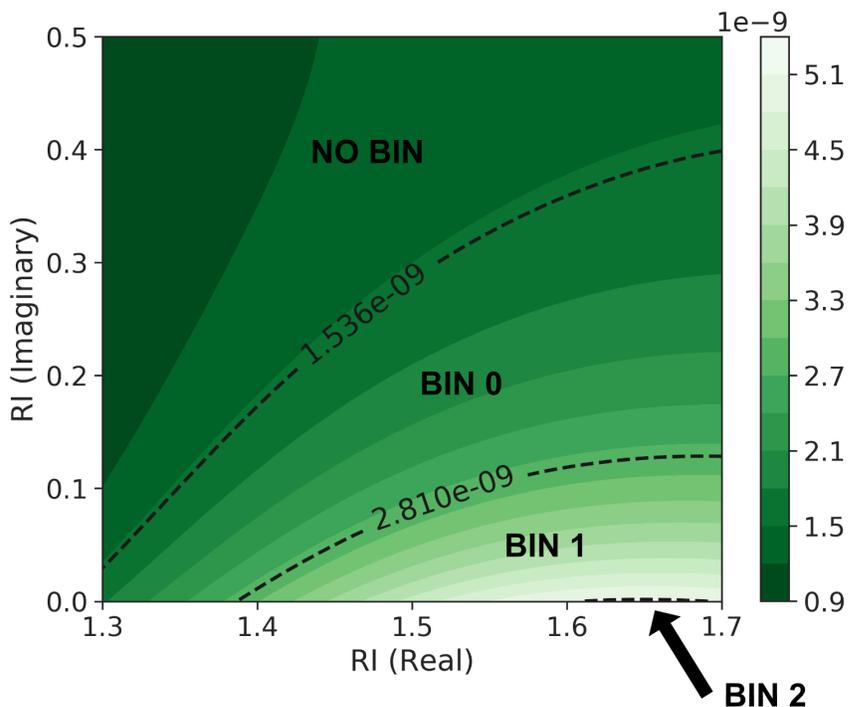


**Figure S2.** Bin assignment as a function of refractive index for a 600 nm particle. An OPC with 16 bins between 380 nm and 17.5  $\mu\text{m}$  and a 658 nm laser calibrated using PSLs was used to generate this data. Data are colored by the computed integrated scattering cross section.

If we complete the same exercise for a 1  $\mu\text{m}$  particle, the results are quite different. Small changes in the absorbing component of the refractive index can lead to large differences in how the particle is assigned to a bin. Over the entire range of optical properties shown in Figure S3, the 1  $\mu\text{m}$  particle can be assigned to 5 different bins (or NO BIN). For this specific OPC, this means the 1  $\mu\text{m}$  particle can be assigned a diameter of anywhere from 0  $\mu\text{m}$  to 1.26  $\mu\text{m}$ . This indicates that for large particles, differences in optical properties of calibration aerosol and measured aerosol can lead to large errors in bin assignments (and hence mass measurements).

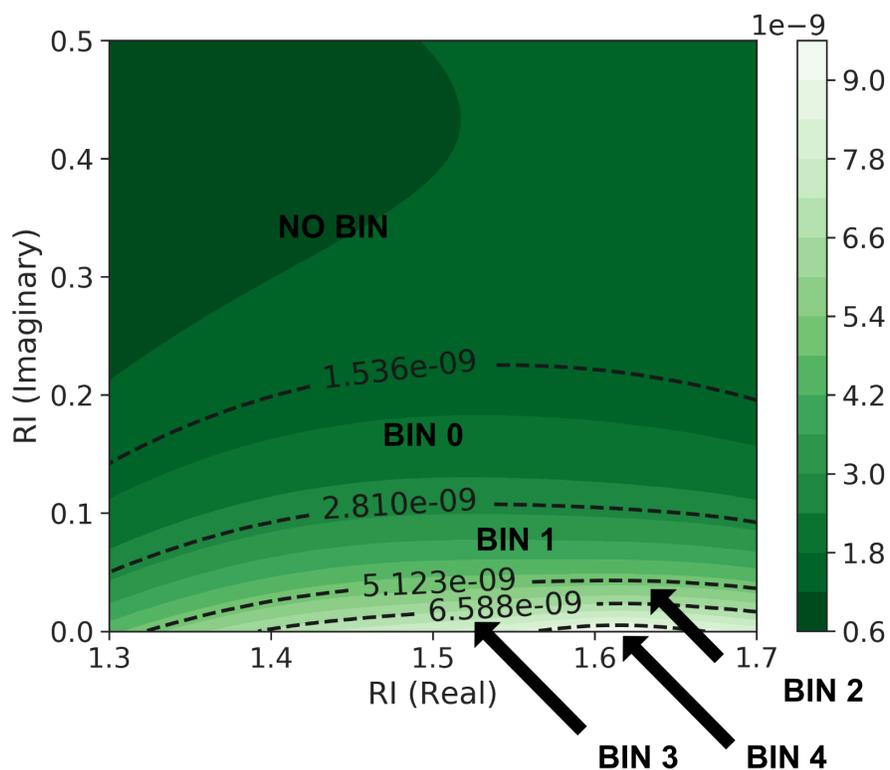


**Figure S3.** Bin assignment as a function of refractive index for a 600 nm particle. An OPC with 16 bins between 380 nm and 17.5  $\mu\text{m}$  and a 658 nm laser calibrated using PSLs was used to generate this data. Data are colored by the computed integrated scattering cross section.

Page 19, line 9: "calibrated using PSL", not ammonium sulfate? (PSL matches the RI in parentheses and the caption of Fig 4.)

Thank you for pointing out this typo – this has been updated in the text.

Pages 24-25: "some proxy for aerosol composition" - In Malings et al. (2019), we used PM composition data from the EPA CSN network (139 sites across the US, Fig S4) with a wide range of chemical composition and found the results did not change significantly (Fig S5), so long as some fRH correction was used. Might be relevant here

This is a very good point made by the reviewer, but that data is not available in real-time, thereby limiting its utility in the context of real-time, low-cost sensor networks. If post-processed data is desired, there are certainly ways to correct the data from low-cost particle sensors for compositional effects. However, this is not a viable approach for real-

time data. To clarify we are referring to real-time corrections, we have changed the text in \_ to read: "...it would be possible to vastly reduce this error and improve the accuracy of mass measurements using OPSs for real-time data collection."

*Page 25, line 11: "therefore" not "therefor"*

This has been corrected.

*Page 25, line 24: are urban OECD aerosol size distributions "highly variable"? This might be another example of "errors that may not be significant in the US/EU but are important in developing countries".*

While the mean aerosol size distribution in OECD countries may be somewhat normalized over time, it is certainly variable on a minute-by-minute (or faster) time basis, which is often the focus of low-cost, real-time air quality sensor networks. To clarify that we were referring to general variability, we have removed the word 'highly' from the text.

*Table 4: some issues with this - "small PSD" or "large PSD" suggests narrow or broad size distribution, but I suspect the authors mean "smaller aerosols" or "larger aerosols". Please clarify.*

We thank the reviewer for pointing this out – we have clarified this in the text by changing "PSD" to "GMD", indicating that we are talking about smaller particle sizes.

*NIST urban aerosol - SRM 1648 was collected in 1976-1977 and may not be representative of, well, anything these days...*

This is an excellent point! We are aware of no other standards for urban aerosol, so we have added "or collected particles" to this entry.

*Maybe the "aerosol properties" column should have some references?*

This column has been updated to include references.

*The authors emphasize this table is only a start, so it's fine to include it, I guess. There could be an entire workshop devoted to Table 4...*

We are in complete agreement. We thank the author for pointing this out and agree that much more could be investigated here; however, as noted above, this is not the focus of this paper and we hope that this will be expanded in the future.

*Throughout: Malings et al. (2019), not Malings et al. (2020). (I don't know why T&F's "download citation" shows the year as 2020. The paper was published in June 2019 and my downloaded PDF shows 2019 as the year for citation.)*

The AS&T special issue on low-cost sensors (Vol. 54 issue 2) was published in 2020, despite the fact that most of the papers were posted online in 2019. Since 2020 is the official publication date, we leave the reference as-is.

*Throughout: "The pluralization of abbreviations, too, requires no apostrophes. More than one CD = CDs... Etc." - Benjamin Dreyer, Dreyer's English (2019). See also: <https://www.chicagomanualofstyle.org/qanda/data/faq/topics/Plurals.html?page=1>*

Thank you for pointing this out – this has been fixed throughout the text.

## Reviewer 3

### Major Comments

*More analysis needs to be done to demonstrate the importance of these factors in measuring real world particles. Examples presented in the text are simple hypothetical cases that just show the importance of each factor. It is important for the reader to see how much the results of actual atmospheric particle measurements get affected by these errors. Analysis of data from previous studies would be helpful to obtain a picture of how much those data would change if corrected for the effects. One major question is to see if the final conclusion from some of previous studies would be affected based on these factors.*

We thank the reviewer for their suggestions (similar to those made by the other two reviewers) and absolutely agree that real-world examples and data analysis would be of interest and importance. We also agree that these examples are purely hypothetical and show the importance of each factor. But this in fact was our objective – our goal was to show the impact of each individual factor via modeling (as opposed to field measurements) for the reasons outlined in the introduction of this paper. Including more real-world data is beyond the scope of this work, but we do plan on follow-up work that compares our modeled results to field measurements for some nephelometers and OPCs and hope others will carry out similar studies for individual use-cases.

*The abstract and introduction create the expectation that this article would also address the interaction between different factors and the impact on accuracy of measurement results. However, presented cases are all single-factor studies. If authors believe the interdependence of these factors is significant, these mutual effects should be addressed in the paper.*

While we examine the different factors individually, many of these interdependencies are actually built in: for example, water uptake affects size as well as density and RI (p. 5, lines

8-11). We did attempt to examine all of these factors in aggregate by varying all of them across atmospherically relevant ranges; but such reasonable ranges can vary dramatically from environment to environment, and the errors were largely a function of the spread in values chosen, and not anything inherent about the sensors themselves. To avoid such ambiguities in ranges of aerosol types, we instead present broad uncertainty ranges from each contributor in Table 3 to give the reader an overall sense of how the different sources of error contribute. To avoid implying in the abstract and introduction that these interdependencies are systematically examined, we have clarified the text in a few places:

P2 line 13: "...is used to estimate the fractional error in mass loading..."

P5 line 8: "...to our knowledge, there has not been a systematic, comprehensive investigation of all these factors together."

## Minor Comments

*Title – "low-cost" word can be omitted from the title as this manuscript looks at low cost as well as "high end" instruments.*

Because the focus and objective of this work is investigating the accuracy of low-cost sensors, we feel it is important to keep the term in the title, even if the work is applicable to higher-fidelity instruments as well.

*P5, L3 – Please provide a brief description of factors resulting in "changes in aerosol optical properties".*

We have changed the text to make this more clear. The text now reads: "...(3) changes in scattering efficiency due to differences in aerosol optical properties; and (4) the need for aerosol-specific correction factors to account for differences in density."

*P8, Table 1 – Have the authors tried contacting the manufacturers to obtain the data that is missing in the literature?*

We had been relying on what was in the literature, but on the reviewer's suggestion, have reached out to the manufacturers. We have not yet received responses but will update the table when/if we do.

*P12, L7 – Why is geometric mean used for mass calculations? Are the authors suggesting that they use the measured pulse heights from individual particles rather than assuming uniform size distribution across each individual size bin? If yes, what is the point of referring to size bins?*

The geometric mean is used for mass calculations because when using an OPC, the exact particle diameters are unknown. Instead, only the number of particles in a given size bin is known. To model the process of an OPC as closely to reality as possible, we take the exact size of a particle, compute its scattering value, and then assign that to a bin, which is the process an actual OPC takes when making measurements. We bin the resulting scattering values in the same way an actual OPC would (an analog-to-digital converter or FPGA would bin them in this context) which is important for understanding small changes in aerosol properties can lead to a particle being sized incorrectly and placed into the wrong bin. Thus, it is quite important that we refer to bins as opposed to the actual size of the particle, as this is how the devices work in reality.

*P12, L24 – Similar comment as above. Please clarify the reason for preferring geometric mean diameter.*

Data from an OPC does not include exact particle diameters and the exact light pulse height is not typically stored. If pulse heights were stored, then theoretically, one could correlate the pulse height to a particle diameter; however, this is not how OPCs typically work. Whether using a low-cost OPC or a reference-grade OPC data is in the form of a histogram where the bins represent a range of particle diameters and the height represents the number of particles or particle number concentration in that size bin. To then compute a mass value, it is necessary to assume some diameter or volume per particle. As mentioned in the paper, this is typically the geometric mean diameter.

*P15, L9-10 – “overestimate” and “underestimate” would be more accurate terms for these sentences.*

This has been corrected to reflect these terms.

*P15, L22-24 – The wording in this section is unclear. Do the authors mean that “very few low cost OPSs control relative humidity. . .”?*

The reviewer was correct – this has been corrected.

*P16, L1- Should read “Figure 2 shows the impact that RH can. . .”*

This has been corrected.

*P17, L20 – Please add more explanation about Mie scattering of black carbon particles in the <300nm range. The trend shown in >300nm range is understandable based on the BC particles being more absorbing, but an explanation for <300nm range is missing.*

BC particles smaller than 300 nm scatter more light than non-BC particles at this size because the scattering component of the refractive index is much higher; for black

carbon, the refractive index is  $1.95 - 0.79j$ . When the particles are smaller, this has a greater effect than the absorbing component, as is discussed in Bohren and Huffman. This effect can also be seen in Figure 3 – the Mie calculations show that BC < 300 nm scatters more light than non-BC particles, but as the absorbing component becomes more relevant as the particles get larger, BC scatters far less light than the non-BC particles.

Fig 5 – Please show the contour line corresponding to  $M_m/M_a=1$

This suggestion has been implemented – there is now a black dashed line indicating the 1:1 line on Figure 5. The image is also re-printed below.

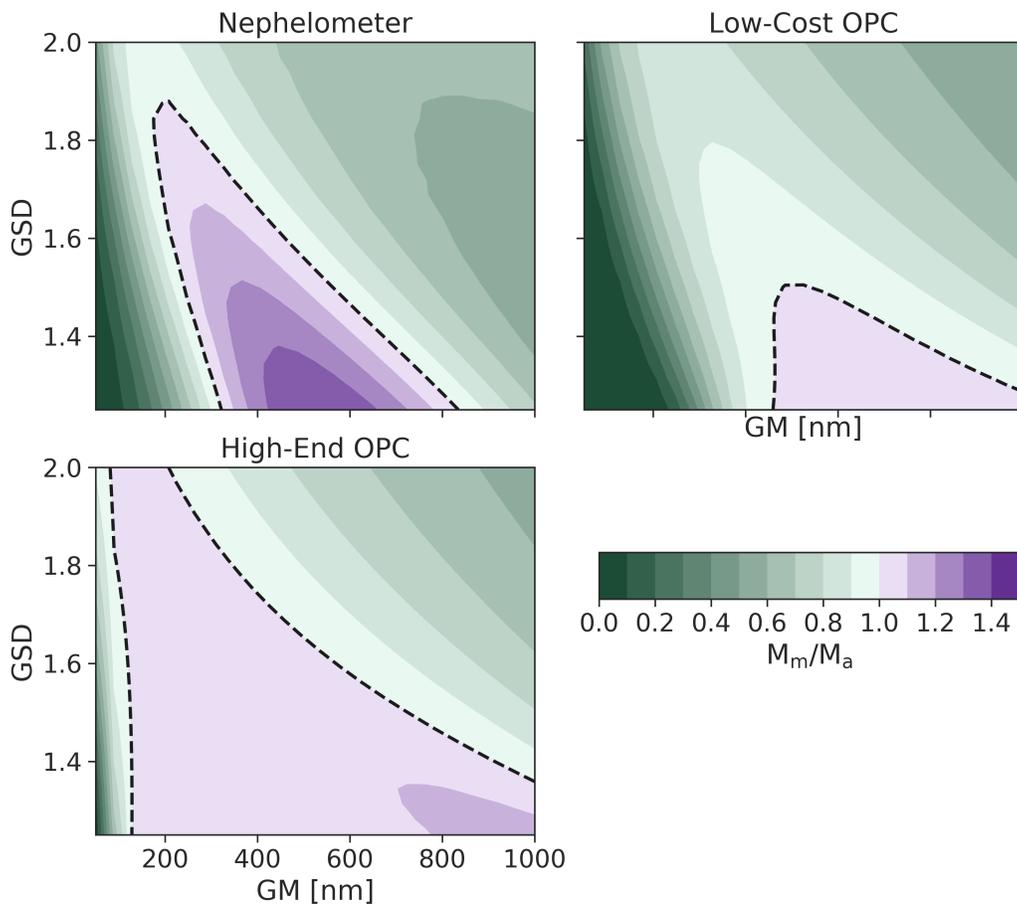


Fig 5 – It seems that even at the calibration conditions ( $GM=400$  nm, and  $GSD=1.65$ ), mass loading accuracy is not equal to unity in any of the plots. What is the explanation?

The OPCs will almost always be unable to see a portion of the size distribution, even if it is very large, as the tail of the distribution will fall below the detectable range of the OPC. This 'missing mass' is discussed throughout the section. As a larger fraction of the size

distribution is within the detectable range of the OPC, the more accurate the device will become. As for the nephelometer, an incorrect refractive index (1.592) was used instead of the listed (ammonium sulfate, 1.521). The figure has been updated. At this distribution, the value is 1 at these conditions and changes as the distribution changes, as is discussed in the section itself.

*Table 4 – Need to mention that the main metric in consideration in this table is mass loading. Clearly, if the focus in a study is on evolution of particle size distribution rather than integral mass loading, nephelometer can't be recommended.*

We have updated the description of the table to make it clear the primary metric is accuracy in mass loading measurement.

1 Assessing the accuracy of low-cost optical particle sensors  
2 using a physics-based approach

3  
4 David H Hagan<sup>1, 2, 3</sup>, Jesse H Kroll<sup>1, 3</sup>

5  
6 <sup>1</sup>Department of Civil and Environmental Engineering, Massachusetts Institute of Technology, Cambridge,  
7 MA 02139, USA

8 <sup>2</sup>QuantAQ, Inc., Somerville, MA 02143, USA

9 <sup>3</sup>Department of Chemical Engineering, Massachusetts Institute of Technology, Cambridge, MA 02139, USA

10  
11 Corresponding Author Emails: david.hagan@quant-aq.com or jhkroll@mit.edu

12  
13  
14  
15

## 1 Abstract

2 Low-cost sensors for measuring particulate matter (PM) offer the ability to understand human  
3 exposure to air pollution at spatiotemporal scales that have previously been impractical. However,  
4 such low-cost PM sensors tend to be poorly characterized, and their measurements of mass  
5 concentration can be subject to considerable error. Recent studies have investigated how individual  
6 factors can contribute to this error, but these studies are largely based on empirical comparisons,  
7 and generally do not examine the role of multiple factors simultaneously. Here, we present a new  
8 physics-based framework and open-source software package (*opcsim*) for evaluating the ability of  
9 low-cost optical particle sensors (optical particle counters and nephelometers) to accurately  
10 characterize the mass loading of aerosol particles. This framework, which uses Mie theory to  
11 calculate the response of a given sensor to a given particle population, is used to estimate the  
12 fractional error in mass loading for different sensor types, given variations in relative humidity,  
13 aerosol optical properties, and the underlying particle size distribution. Results indicate that such  
14 error, which can be substantial, is dependent on the sensor technology (nephelometer vs. optical  
15 particle counter), the specific parameters of the individual sensor, and differences between the  
16 aerosol used to calibrate the sensor and the aerosol being measured. We conclude with a summary  
17 of likely sources of error for different sensor types, environmental conditions, and particle classes,  
18 and offer general recommendations for choice of calibrant under different measurement scenarios.

19

## 20 1. Introduction

21 Human exposure to aerosols is associated with adverse health impacts and increased mortality  
22 (Apte et al., 2018; Burnett et al., 2018; Cohen et al., 2017; Dockery et al., 1993). The source and  
23 composition of aerosols has been linked to a range of negative health impacts (Antonini et al.,  
24 2003; Hart et al., 2012; Henneberger and Attfield, 1997; Lipsett and Campleman, 1999), with  
25 more than 4 million annual deaths worldwide attributed to ambient particulate matter pollution  
26 (Cohen et al., 2017). Accurate estimates of aerosol sources and health impacts rely critically on  
27 measurements of particulate matter mass concentrations across indoor and outdoor  
28 environments worldwide.

29

30 In many countries, particulate matter (PM) pollution is regulated by national or local government  
31 agencies (e.g., the US EPA in the United States) and is typically measured using federally approved

1 reference methods that are high in accuracy and precision. The existing infrastructure is generally  
2 designed to measure regional-scale air pollution, in order to enforce (and assess the effectiveness  
3 of) air quality regulations. However, particle pollution can vary in space and time at much finer  
4 resolution than can be measured using standard monitoring technologies, due to their relatively  
5 high cost and size. Over the past several years, new technologies have emerged at price points  
6 (<\$2000) that allow PM measurements to be made with much higher spatiotemporal resolution,  
7 even down to the individual human level (Koehler et al., 2019; Tryner et al., 2019a, 2019b). These  
8 devices are physically small, use very little power, and can easily be deployed at scale. As a result,  
9 such sensors are ideally suited for use in dense distributed sensor networks, providing high-  
10 resolution air quality measurements, as well in as personal monitoring, providing individuals with  
11 the ability to measure and understand their exposure to harmful air pollutants. As with all low-  
12 cost sensors (LCS), accuracy is of paramount concern; as shown by a number of recent laboratory  
13 and field-based evaluation studies (Crilley et al., 2018; Dacunto et al., 2015; Di Antonio et al.,  
14 2018; Holstius et al., 2014; Levy Zamora et al., 2019; Malings et al., 2020; Northcross et al., 2013;  
15 Sousan et al., 2016b, 2016a; Wang et al., 2015), PM sensors can perform quite poorly without  
16 additional constraints or calibrations.

17  
18 Most low-cost PM sensors measure particles via light scattering. Sampled particles intercept a  
19 beam of light (typically from a laser or LED with a wavelength between 405 and 780 nm), and the  
20 scattered light is measured and correlated to a PM mass concentration. In this work, we refer to  
21 such instruments as optical particle sensors (OPSS). OPSS can be broken down into two main  
22 types, nephelometers and optical particle counters (OPCs). Nephelometers measure the particles  
23 as an ensemble, gathering light scattered by all particles across a wide range of angles, typically  
24 7°-173° to avoid pure forward and backward scattering (Abu-Rahmah et al., 2006; Ahlquist and  
25 Charlson, 1967; Anderson et al., 1996). The total scattering amplitude is then correlated to a mass  
26 measurement made by a reference instrument. (Nephelometers that measure scattered light at  
27 a single angle are sometimes referred to as photometers; for the purposes of this work we  
28 consider photometers to be a subclass of nephelometer.) OPCs, by contrast, detect particles  
29 individually, providing information on their number and size. Light scattered by each individual

1 particle is measured and each pulse is assigned to a size bin based on its total light intensity,  
2 resulting in a histogram which is converted to a mass loading once the entire distribution has  
3 been measured. While these technologies have been around for decades (Gucker et al., 1947;  
4 Patterson et al., 1926), they have recently become available at much lower cost due to the  
5 availability of small, inexpensive light sources and electronic components.

6

7 The use of light scattering introduces a number of fundamental limitations for making PM mass  
8 measurements. Many of these arise from environmental conditions and/or the properties of the  
9 aerosol being measured; these can be especially problematic when calibration is done using only  
10 a single aerosol type or condition. A number of recent empirical studies of **OPs** have investigated  
11 some of these limitations. These issues include: (1) the inability to adapt to changes in the particle  
12 size distribution (Dacunto et al., 2015; Wang et al., 2015); (2) the hygroscopic growth of particles  
13 due to changes in ambient relative humidity (Crilley et al., 2018; Di Antonio et al., 2018; Malings  
14 et al., 2020; Zheng et al., 2018); (3) changes in scattering efficiency due to **differences** in aerosol  
15 optical properties (Crilley et al., 2018; Di Antonio et al., 2018); and (4) the need for aerosol-  
16 specific correction factors to account for differences in density (Dacunto et al., 2015; Northcross  
17 et al., 2013). While these studies have examined how these individual effects in isolation may  
18 affect PM accuracy, to our knowledge there has not been a systematic, comprehensive  
19 investigation of all these **factors together**. Complicating matters is the fact that these individual  
20 properties are all intertwined – for example, when relative humidity increases, it can cause  
21 particles to take up water, which can change not only their size and mass but also their shape,  
22 refractive index, and density.

23

24 To **examine the** relative contribution of error by these **various sources**, we have developed a  
25 model that describes how a given sensor will respond to different aerosols **under a wide range**  
26 **of conditions**. This model is based entirely on the underlying physics of light scattering (Mie  
27 Theory) rather than empirical relationships obtained through laboratory or field measurements.  
28 While previous work has modeled nephelometers and **OPCs** in a similar way (Walser et al., 2017),  
29 we believe this is the first detailed treatment of light scattering as it relates specifically to LCS.

1 We use this model to isolate the relevant sources of error and develop a better understanding of  
2 the limitations (as well as strengths) of different kinds of OPSSs.

3  
4 The modeling tool described here, which is open source and freely available, can be used for the  
5 systematic study of how different OPSSs may detect various aerosol types under a range of  
6 environmental conditions. This enables new insights into the potential errors associated with a  
7 given PM measurement, optimal strategies for calibrating OPSSs, the development of algorithms  
8 for data analysis, and ultimately in the design of the sensors themselves. The objective of this  
9 work is to describe the model and software and to investigate broad influences on aerosol  
10 properties and sensor parameters on measurement performance. We do not investigate the  
11 performance of individual commercially available sensors under the full range of conditions  
12 expected in the atmosphere; but such studies are enabled by this modeling tool and are an  
13 important future extension of this work.

## 14 2. Methods

15 The modeling framework described in this section is available as an open-source (MIT license)  
16 python library (*opcsim*) and has been made available on GitHub. Detailed documentation,  
17 including installation instructions and examples, are available online (Hagan and Kroll, 2019). The  
18 framework, called “opcsim”, consists of two primary components: the code that models OPSSs  
19 and implements the Mie Theory algorithms (Bohren and Huffman, 1983; Sumlin et al., 2018), and  
20 the code to build and evaluate aerosol distributions.

21  
22 We follow the same general modeling pattern regardless of sensor type. Steps include: (1)  
23 defining the device based on its key physical parameters; (2) calibrating the device to a specific  
24 aerosol type (for OPCs) or aerosol distribution (for nephelometers); and (3) evaluating each  
25 particle in an aerosol population by computing the scattered light signal using Mie theory and  
26 converting that signal to the sensor output based on its calibration. In the following sections we  
27 describe how the aerosol population is described by the model, followed by how the sensors  
28 themselves are treated.

29

1    2.1        Representing an aerosol distribution

2    We represent an aerosol distribution as the sum of  $n$  lognormal modes, where each mode  $i$  is  
3    defined by its geometric mean particle diameter ( $\bar{D}_{pi}$ ), geometric standard deviation ( $\sigma_i$ ), and  
4    number concentration ( $N_i$ ). The aerosol distribution as a function of diameter  $D_p$  ( $dN/d\log D_p$ ) is  
5    given by Equation 1 (Seinfeld and Pandis, 2006):

6

$$\frac{dN}{d\log D_p} = \sum_{i=1}^n \frac{N_i}{\sqrt{2\pi} \log \sigma_i} \exp\left(-\frac{(\log D_p - \log \bar{D}_{pi})^2}{2 \log^2 \sigma_i}\right) \quad \text{(Equation 1)}$$

7

8

9    Additionally, we define the composition of the aerosol distribution by defining the particle  
10    density ( $\rho_i$ ), hygroscopic growth factor ( $\kappa_i$ ), and complex refractive index ( $m_i$ ) for each mode. The  
11    role of these additional parameters is discussed in section 3, below. While more complex  
12    representations of the chemical makeup of the aerosol can be implemented using our modeling  
13    framework (i.e., core-shell representation of aerosols, complex aerosol mixtures, etc.), for the  
14    purposes of this manuscript we focus only on well-mixed homogeneous particle modes, as  
15    described by Eq. 1. The above number distribution can be converted to a mass distribution (or  
16    total mass concentration) by assuming all particles are spherical with a known density (Seinfeld  
17    and Pandis, 2006).

18

19

20    2.2        Representing Optical Particle Sensors

21    2.2.1      Optical Particle Counters (OPCs)

22    An OPC is defined by three instrument-specific parameters: (1) the wavelength of the light source  
23    ( $\lambda$ ), (2) the viewing angle for which the scattered light is collected, and (3) the number of discrete  
24    size bins and their widths. A bin, in this context, refers to a single “slice” of the aerosol size  
25    distribution, with a fixed width and units of particle diameter. Typically, most low-cost OPCs have  
26    between 2-30 bins. These can be determined either by looking up the parameters in the device’s  
27    datasheet provided by the manufacturer or by making simple measurements. Bins are often  
28    chosen to reduce the uncertainty in correct bin assignments within the bounds of what the sensor

1 is capable of detecting. Most low-cost OPCs have the smallest bin at  $D_{\min} \sim 500$  nm, with cost  
 2 typically being the driving factor – OPCs with lower  $D_{\min}$  employ more expensive, higher-quality  
 3 optics and photodetectors, allowing them to detect smaller particles. In this work, the bin  
 4 boundaries (and hence widths) used for a given OPC are taken from the manufacturer’s spec  
 5 sheets, if available; otherwise they are calculated by generating an array of logarithmically-  
 6 spaced bin boundaries for a set number of bins ( $n_{\text{bins}}$ ) between the minimum and maximum  
 7 defined diameters ( $D_{\min}$  and  $D_{\max}$ , respectively). Most often, a light pulse generated by a single  
 8 particle is assigned to exactly one bin; however, there exist approaches where bin assignments  
 9 are made using a probability distribution (Walser et al., 2017); this is not implemented in this  
 10 model but is an approach that could be added in the future.. Table 1 lists bin widths and other  
 11 parameters for a few commercially available low-cost OPCs.

12  
 13 **Table 1.** Characteristics of a selection of commercially available low-cost optical particle counters and  
 14 nephelometers.

Manufacturer	OPS Type	Model	$\lambda$ (nm)	Viewing Angle ( $\phi_1, \phi_2$ )	# of Size Bins
Alphasense, Ltd.	OPC	OPC-N2	658	(32.0°, 88.0°)	16 (0.38 – 17.5 $\mu\text{m}$ )
Alphasense, Ltd.	OPC	OPC-N3	658	(32.0°, 88.0°)	24 (0.35 – 40.0 $\mu\text{m}$ )
Particle Plus	OPC		785	(58.0°, 118.0°)	6 (0.3 – 10.0 $\mu\text{m}$ )
NOAA/Handix	OPC	POPS	405	(38.0°, 142.0°)	16 (0.132 – 3.65 $\mu\text{m}$ )
Plantower	Nephelometer	PMS5003	$\sim 650$	? <sup>1</sup>	6 (0.3 – 10+ $\mu\text{m}$ ) <sup>2</sup>
Sharp	Nephelometer (Photometer)	GP2Y1010AUOF	870- 980	? <sup>1</sup>	1 (?) <sup>1</sup>
Shinyei	Nephelometer (Photometer)	PPD42NS	870- 980	? <sup>1</sup>	1 (>1 $\mu\text{m}$ )
Samyoung	Nephelometer (Photometer)	DSM501A	870- 980	? <sup>1</sup>	1 (>1 $\mu\text{m}$ )

15 <sup>1</sup> Unknown; not provided in the manufacturer’s technical data sheet or the technical literature

16 <sup>2</sup> The PMS5003 reports six bins; however these are not actual size bins, but rather software-computed  
 17 results (He et al., 2020).

1  
2 **OPCs** are calibrated by relating the scattered light intensity – a combination of the particle’s  
3 scattering cross section ( $C_{scat}$ ) and laser intensity – to the particle diameter. Practically, this is  
4 done by using calibration aerosols with known optical properties and size and generating a  
5 calibration curve between the test aerosol and the electronic pulse height generated by that  
6 aerosol. After repeating this process for many sizes, a calibration curve can be generated. Here,  
7 we compute the  $C_{scat}$  values using Mie theory using attributes of the calibration aerosol. To  
8 simplify the model, we make several assumptions, including: (1) all particles are spherical and  
9 homogeneous (well-mixed); (2) the laser intensity is constant, implying all particles are perfectly  
10 centered in the beam of the laser; and (3) the photodetector and electronics are 100% efficient,  
11 and so we do not consider the impact of signal-to-noise limitations.

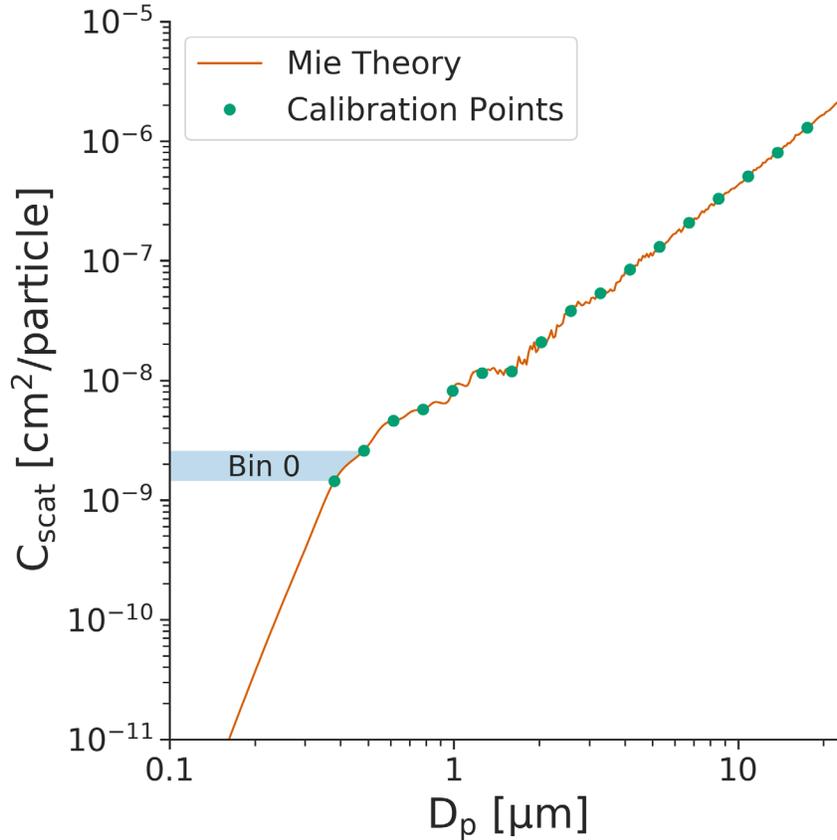
12  
13 As most low-cost **OPCs** contain an elliptical re-focusing mirror to gather the scattered light across  
14 many angles, we compute the integrated light scattering intensity following a procedure first  
15 introduced by Jaenicke and Hanusch (Jaenicke and Hanusch, 1993). Mie theory calculations are  
16 implemented using equations by Bohren and Huffman (Bohren and Huffman, 1983). The  
17 scattering cross-section is calculated as:

18  
19 
$$C_{scat} = \frac{\lambda}{4\pi} \int_{\theta_1}^{\theta_2} [i_1(\theta) + i_2(\theta)] \sin\theta \, d\theta \quad (\text{Equation 2})$$

20  
21 where  $\lambda$  is the wavelength of incident light,  $\theta$  is the viewing angle (which ranges from  $\theta_1$  to  $\theta_2$ ),  
22 and  $i_1$  and  $i_2$  are the intensity distribution functions (Bohren and Huffman, 1983).

23  
24 Figure 1 depicts the calibration curve generated for an OPC with the characteristics of the  
25 Alphasense OPC-N2 (Table 1), using polystyrene latex spheres (**PSLs**) of different diameters for  
26 calibration. Eq. 2 was used to compute the theoretical  $C_{scat}$  values (y axis), integrated across the  
27 entire viewing angle, for a range of particle diameters (x axis). The  $C_{scat}$  values at each bin  
28 boundary (green dots in Fig. 1) are then computed, and spline interpolation is used between each  
29 individual bin boundary to generate a mapping between the scattering amplitude and its

1 corresponding bin assignment. In practice, this operates as a lookup table – a particle crossing  
2 the laser generates a scattering amplitude which is associated with a specific ‘bin’ via the  
3 calibration.



4  
5 **Figure 1.** Calibration data for an OPC with 16 discrete size bins between 0.38 – 17.5  $\mu\text{m}$ . OPC parameters  
6 were chosen to match the Alphasense OPC-N2 (wavelength of 658 nm, viewing angle of 32-88°) using  
7 monodispersed polystyrene latex spheres ( $m = 1.592 + 0j$ ). The integrated scattering amplitude  
8 calculated using Mie theory is shown as the solid line, with points depicting the corresponding scattering  
9 amplitude at each of the bin boundaries. Shown as a shaded box is the range of scattering amplitudes that  
10 is assigned to the smallest size bin.

11  
12 For **OPCs** that measure scattered light across a wide angle,  $C_{\text{scat}}$  is generally a monotonically  
13 increasing function of the particle size. However, there may be cases where this is not true,  
14 typically due to the presence of Mie resonance (e.g., near  $D_p=1.5 \mu\text{m}$  in Fig. 1). When the function  
15 is not monotonic, we apply a smoothing algorithm (Cerni, 1983; Osborne et al., 2008) or merge  
16 together multiple bins (Pinnick et al., 1981; Walser et al., 2017) and accept the tradeoff where  
17 we obtain a higher rate of correct bin assignment in exchange for reduced bin resolution. This

1 non-monotonicity is less of an issue as the viewing angle becomes wider, as the larger range of  
2 angles will “smooth out” any Mie resonances (Figure S1). The wide viewing angle thus offers two  
3 key advantages: (1) the total signal (pulse height) is larger, making it easier to detect small  
4 particles using inexpensive electronics; (2) the calibration curve is less susceptible to small  
5 changes in particle scattering cross-section.

6  
7 While an OPC sizes and counts individual particles, we generally are interested in evaluating the  
8 entire population of particles. To obtain the results for the entire population, we compute the  
9 scattering cross-section for each particle in the distribution, and assign it to a bin using the  
10 calibration curve generated previously – this results in a histogram with the total sum of particles  
11 in each discrete size bin over a period of time. Once we have the number distribution, we can  
12 compute the aerosol mass loading (PM) using Eq. (3):

13  
14 
$$PM = \rho \sum_i N_i \frac{\pi}{6} D_{p,i}^3 \quad (\text{Equation 3})$$

15  
16 where  $N_i$  is the number concentration for a given size bin,  $D_{p,i}$  is the geometric mean diameter  
17 for a given size bin, and  $\rho$  is the particle density, chosen to be constant. We can integrate mass  
18 loadings between different diameters by summing only across a sub-selection of bins (for  
19 example, if we intend to calculate the  $PM_1$  mass concentration, we would choose only the size  
20 bins corresponding to particles sized between 0-1  $\mu\text{m}$ , whereas to calculate the  $PM_{2.5}$  mass  
21 concentration, we would use the bins corresponding to sizes between 0-2.5  $\mu\text{m}$ ). This approach  
22 for computing mass loadings is similar to that used by others (Di Antonio et al., 2018), though we  
23 use the geometric mean particle diameter as opposed to the mean particle diameter.

24  
25 **2.2.2 Integrating nephelometers**

26 Nephelometers gather the light scattered by an aerosol population across a wide range of angles  
27 to gather as much of the scattered light as possible, while avoiding the near-forward and near-  
28 backward scattered light. Here, we define a nephelometer by the wavelength of its light source  
29 ( $\lambda$ ) and its viewing angle.

1

2 In practice, nephelometers are calibrated empirically by correlating the total scattered light signal  
3 to a reference mass measurement (Dacunto et al., 2015; Sousan et al., 2016b; Wang et al., 2015).

4 Within our model, we do the same by computing the total scattered light signal using Mie theory  
5 and then take the ratio of the scattered light to a calculated mass loading. The total scattered

6 light signal is calculated by integrating Eq. 2 across the entire particle size distribution, resulting  
7 in a single scattered light intensity for a given aerosol distribution. The calibration factor is then

8 calculated by taking the ratio of this value and the mass loading of the aerosol distribution, which  
9 is calculated by integrating the volume distribution and multiplying by the particle density

10 (Equation 3). Once we have computed the calibration factor, we can calculate the mass loading  
11 for any aerosol distribution by multiplying the calibration factor by the calculated total scattered

12 light signal.

13

### 14 3. Results and discussion

15 We use the model described above to isolate the relative source of error associated with various  
16 differences in physical and optical properties of aerosols, as well as with the devices themselves.

17 We include both simple, targeted experiments probing the effects of changes in isolated  
18 properties, as well as more complex, realistic experiments that attempt to mimic real-world

19 scenarios. In the latter case, we include a variety of aerosol types in our model runs to resemble  
20 real-world use-cases; aerosol types include urban aerosol, wildfire emissions, marine aerosol,

21 dust, and continental background. The physical and optical properties for these aerosols are  
22 summarized in Table 2. We discuss these results in the context of three particle sensors chosen

23 to be representative of low-cost OPSs: a nephelometer, which uses a 658 nm light source and has  
24 a viewing range of 7°-173°, and two OPCs, both with 16 equally-spaced bins, a 658 nm light

25 source, and a viewing angle of 32-88°. The two OPCs differ only in the minimum particle size  
26 measured: the ‘low-cost OPC’ is representative of commercial OPCs currently on the market and

27 measures particles in the 0.38-17.5  $\mu\text{m}$  size range; and the ‘high-end OPC’, representing an  
28 idealized OPC that can measure much smaller particles, with a detection range of 0.1-17.5  $\mu\text{m}$ .

1 We note that many expensive OPCs cannot measure particles down to 100 nm; this lower size  
 2 cutoff was chosen as an approximate smallest particle size that an optical sensor can detect.

3

4 **Table 2.** Aerosol optical and chemical properties used in this work.

Aerosol Type	Refractive index	Hygroscopicity parameter $\kappa^6$	Density (g cm <sup>-3</sup> )
Urban <sup>1</sup>	1.525+0.020j	0.40	1.35
Background <sup>2</sup>	1.520+0.008j	0.25	1.45
Marine <sup>3</sup>	1.384+0.001j	1.10	2.16
Dust <sup>4</sup>	1.555+0.003j	0.03	2.60
Wildfire <sup>5</sup>	1.570+0.002j	0.10	1.58

5

6 <sup>1</sup> (Chen et al., 2019; Cheung et al., 2019; Hussein et al., 2004; Jurányi et al., 2013; Raut and  
 7 Chazette, 2007; Rissler et al., 2014; Shepherd et al., 2018; Wehner and Wiedensohler, 2003)

8 <sup>2</sup> (Levoni et al., 1997; Wang et al., 2014; Yin et al., 2015)

9 <sup>3</sup> (Levoni et al., 1997; Ueda et al., 2016; Zieger et al., 2017)

10 <sup>4</sup> (Koehler et al., 2009; Petzold et al., 2009; Rocha-Lima et al., 2018)

11 <sup>5</sup> (Bougiatioti et al., 2016; Laing et al., 2016; McMeeking, 2004; Shepherd et al., 2018)

12 <sup>6</sup> (Petters and Kreidenweis, 2007)

13

14 We begin by investigating the impact that water uptake, driven by changes in the ambient  
 15 relative humidity, has on the ability of all three **OPSS** to infer PM<sub>2.5</sub> mass. Next, we explore the  
 16 impact of aerosol optical properties (namely, the complex RI), followed by the impact that  
 17 perturbations in the underlying particle size distribution can have in the OPS's ability to infer  
 18 mass loadings. Finally, we summarize our results into general recommendations about each OPS  
 19 type. Throughout, to provide a simple metric for the accuracy of OPS measurements, we present  
 20 our results in terms of the ratio of the inferred or measured PM<sub>2.5</sub> mass concentration (M<sub>m</sub>) to  
 21 the actual PM<sub>2.5</sub> mass concentration (M<sub>a</sub>) at 0% relative humidity. An M<sub>m</sub>/M<sub>a</sub> ratio of greater than  
 22 one implies we are **overestimating** the PM<sub>2.5</sub> loading, whereas a value less than one implies we  
 23 are **underestimating** it.

24

### 25 3.1 Relative humidity and hygroscopic growth

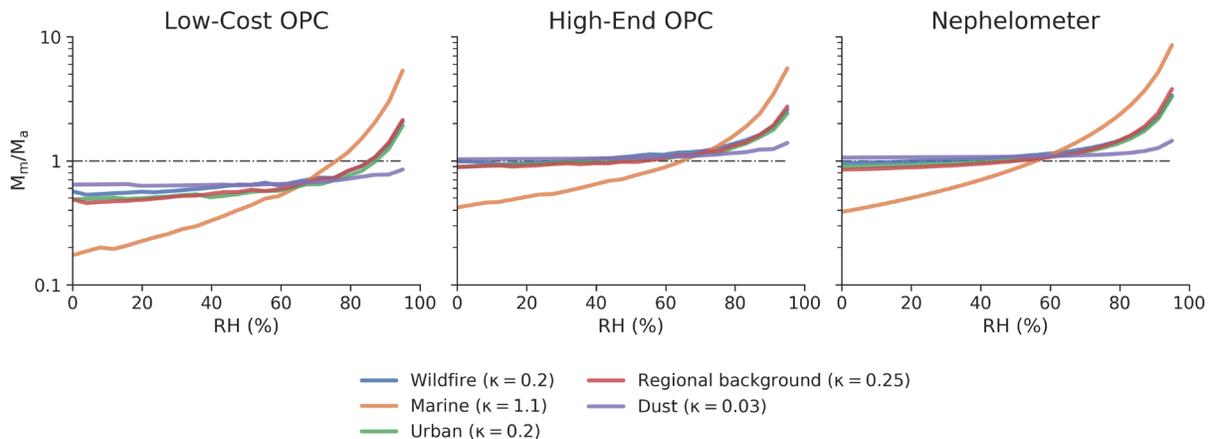
26 One of the most widely discussed sources of error for OPS measurements is that caused by water  
 27 uptake (Crilley et al., 2018; Di Antonio et al., 2018; Malings et al., 2020; Wang et al., 2015; Zheng

1 et al., 2018). As relative humidity increases, hygroscopic particles (those with non-zero  
2 hygroscopic growth parameters,  $\kappa$ ) become larger as they take up water (Petters and  
3 Kreidenweis, 2007), leading to an increase in scattering caused by their increase in size.  
4 Additionally, water uptake changes the optical and chemical properties of the aerosol (e.g., RI,  
5 density, etc.), which can complicate any corrections. The EPA requires PM<sub>2.5</sub> measurements to  
6 be made at relative humidities between 30-40% (Chow and Watson, 1998) to minimize the  
7 effects of hygroscopic growth on samples; however, since very few low-cost OPSs control for  
8 relative humidity (for example, with an in-line dryer), this can often lead to discrepancies when  
9 performing a calibration by co-location or when comparing results between instrument types.

10  
11 Figure 2 shows the impact that RH can have on the accuracy of an OPS. There is little effect until  
12 relative humidity reaches the deliquescence point of the aerosol, which depends on aerosol  
13 composition. At higher relative humidities, OPSs will tend to overestimate PM<sub>2.5</sub> mass, especially  
14 for aerosols comprised of hygroscopic materials. When relative humidity approaches 95%, such  
15 overestimates in PM<sub>2.5</sub> mass become exceedingly large: the OPCs observe a similar effect, with  
16 errors ranging from 100%-500% depending on the hygroscopicity of the aerosol. Nephelometers  
17 see a more pronounced effect with errors as high as 750% for extremely hygroscopic aerosols  
18 and 200%-300% errors for less hygroscopic aerosols.

19  
20 The larger error of the nephelometer is caused in part by the fact that the inferred PM<sub>2.5</sub> mass is  
21 directly proportional to the total scattered light, which has no upper limit. For the OPCs, particles  
22 that take up significant water can be assigned to larger size bins and thus will not be integrated  
23 in the PM<sub>2.5</sub> mass calculation. At moderate humidities (50%-80%), errors for both the  
24 nephelometers and OPCs can vary by as much as 20%-50%, which is in agreement other published  
25 experimental studies on the subject (Crilley et al., 2018; Di Antonio et al., 2018; Malings et al.,  
26 2020; Zheng et al., 2018). In addition to overestimating mass loadings at high relative humidity  
27 due to hygroscopic growth, the OPCs underestimate the mass loadings across all relative  
28 humidities. This is not caused by relative humidity or a lack of hygroscopic growth, but instead is  
29 a result of the “missing mass” below the detectable threshold of the OPC. The low-cost OPC,

1 which cannot detect particles smaller than 380 nm, misses between 30%-90% of the mass,  
 2 whereas the high-end OPC, which can detect particles larger than 100 nm, misses very little mass  
 3 for most aerosol types. The only exception is the marine aerosol, which has a refractive index  
 4 that is substantially different than the aerosol with which the instrument was calibrated.  
 5

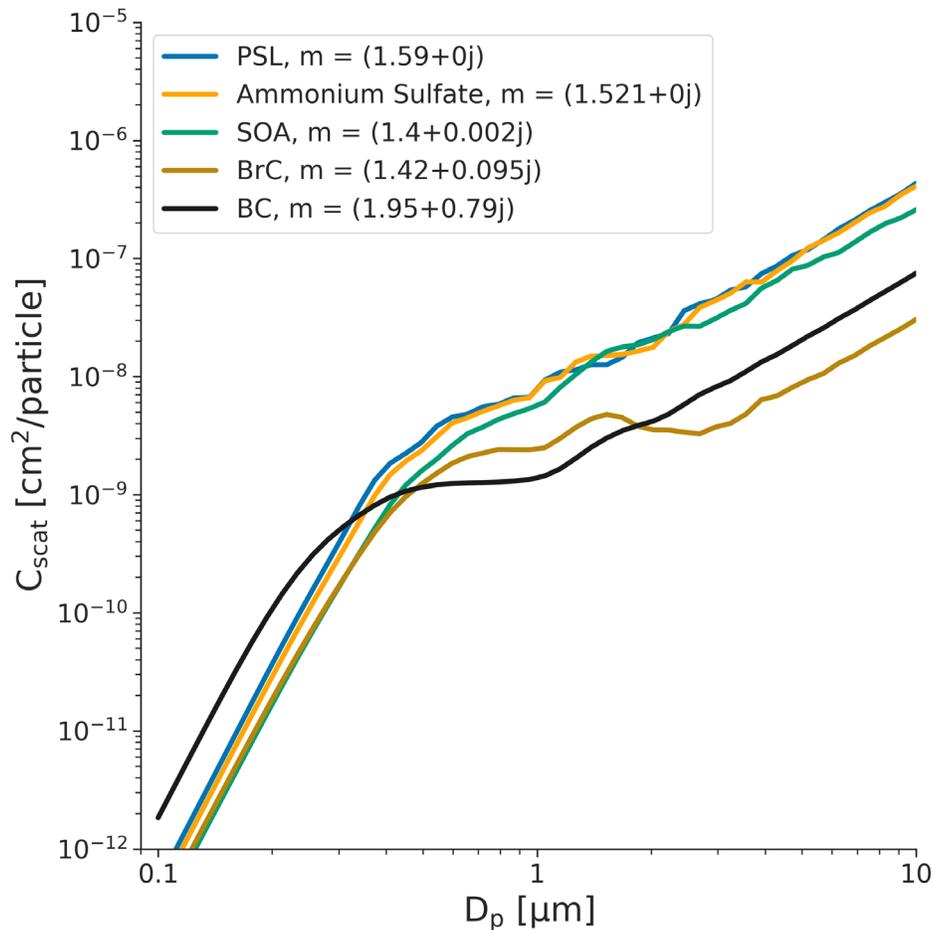


6  
 7 **Figure 2.** The accuracy in  $PM_{2.5}$  mass loading for a given particle sensor ( $M_m/M_a$ ) as a function of relative  
 8 humidity, for common aerosol types. All three particle sensors were calibrated with ammonium sulfate  
 9 (number-weighted Geometric Mean (GM) = 200 nm, Geometric Standard Deviation (GSD) = 1.65). Details  
 10 on the physical and optical properties of the various aerosols can be found in Table 2.

11  
 12 **3.2 Choice of calibration material and aerosol optical properties**

13 **OPCs** are calibrated by correlating the scattering amplitude of known particle sizes for a particles  
 14 of a given composition (Gao et al., 2013). The relationship between scattering amplitude and bin  
 15 assignment (i.e., particle size) is heavily dependent on the aerosol's complex refractive index (RI).  
 16 Figure 3 shows the Mie scattering curve for a range of common calibration materials, including  
 17 both absorbing and non-absorbing materials. For a given particle size, the RI of the particle can  
 18 result in a range of scattered light intensities ( $C_{scat}$ ) that vary by as much as an order of magnitude.  
 19 This can have pronounced effects on the calculated size (and hence mass) of a particle. In  
 20 particular, the Mie curve for black carbon (BC) is substantially different than those of non-  
 21 absorbing materials, with higher real (scattering) and imaginary (absorbing) components. As a  
 22 result, for an OPC calibrated with a non-absorbing material (such as PSLs), smaller BC particles

1 (diameters < 300 nm) will be overestimated in size (due to higher scattering), whereas larger BC  
2 particles (> 300 nm) will be underestimated (due to absorption) (Bohren and Huffman, 1983).  
3  
4 Even small changes in the scattering (real) component of the RI of the calibration material can  
5 lead to particles being assigned to the incorrect bin: an RI higher than that of the calibration  
6 material will generally cause particles to be assigned to bins that are too large (overestimating in  
7 size and mass), and an RI lower than that of the calibration material will generally cause particles  
8 will be assigned to bins that are too small (underestimating in size and mass). This effect is  
9 examined in greater detail in the Supporting Information (Figs S2 and S3). Considering that bins  
10 are often hundreds of nm in width, the impact of such bin mis-assignment on reported mass can  
11 be large. For both OPCs and nephelometers, this will lead to large errors in inferred mass, though  
12 it can be more pronounced for OPCs, since the error for nephelometers is proportional to the  
13 increase in scattering and is not affected by the mis-assignment of individual particles to a  
14 particular size bin.

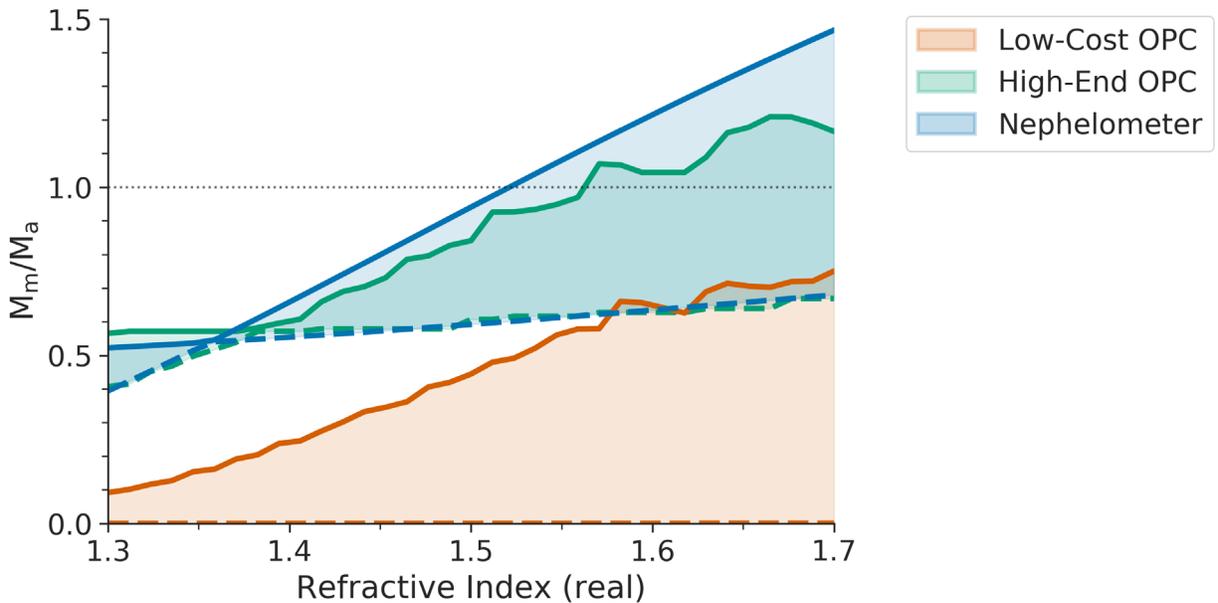


1  
 2 **Figure 3.** Mie curves (integrated over a viewing angle of 32°-88°) for a select group of common calibration  
 3 materials. Materials shown include polystyrene latex spheres (PSLs), ammonium sulfate, secondary  
 4 organic aerosol (SOA), and black carbon (BC). Small differences in the refractive index of a measured  
 5 material can lead to drastic bin mis-assignment (see SI), depending on where bin boundaries are set at  
 6 the time of calibration.

7  
 8 The effect of differences in refractive index on inferred PM<sub>2.5</sub> mass measurements is shown in  
 9 Fig. 4. Results are shown for a single aerosol distribution, in which the only parameter allowed to  
 10 vary is the RI. The real component of the refractive index is shown on the x axis, with the upper  
 11 and lower bounds being determined by the imaginary part of the refractive index; the imaginary  
 12 component ranges from 0 (non-absorbing) to 0.79 (black carbon). The nephelometer (blue  
 13 swatch in Fig. 4) is calibrated using ammonium sulfate ( $m = 1.521 + 0j$ ). When the  
 14 nephelometer is evaluated at this exact RI (and a constant size distribution), it measures mass  
 15 accurately ( $M_m/M_a = 1$ ). However, if the real component of the aerosol being evaluated is higher  
 16 than that of the calibration standard, the total scattering is greater, resulting in the inferred PM<sub>2.5</sub>

1 mass being larger than the actual  $PM_{2.5}$  mass ( $M_m/M_a > 1$ ). Similarly, as the absorbing component  
2 becomes larger, less of the incoming light is scattered, resulting in a substantial underestimation  
3 of the mass loading.

4  
5



6

7 **Figure 4.** The accuracy of **OPs** as a function of the refractive index of the aerosol being measured. The  
8 real component of the RI is on the x axis, and the width of each swatch bounded by the  
9 absorption/imaginary component, which spans from 0 (non-absorbing, solid line) to 0.79 (black carbon,  
10 dashed line). Results are shown for a nephelometer (blue), and the two **OPs** (orange and green). All  
11 results are for a generic particle size distribution with number-weighted GM=200 nm and GSD=1.65 and  
12 the **OPs** were calibrated with **PSLs** whereas the nephelometer was calibrated with ammonium sulfate.

13

14 Also shown are the results for two **OPs**. The high-end OPC (green) is sensitive to particles as  
15 small as 100 nm, whereas the low-cost OPC (red) is sensitive to particles as small as 380 nm. As  
16 the absorbing component of the refractive index becomes larger, the scattering amplitude across  
17 the entire distribution is too small for the OPC to detect, resulting in a mass reading of zero. Both  
18 **OPs** exhibit this effect, but for the high-end OPC, fewer particles will fall below the size cutoff  
19 of the OPC than for the low-cost OPC, resulting in a less dramatic underestimation of the mass.  
20 Most commercially available OPCs are more similar to the low-cost OPC, with lower limits of  
21 detection of around 500 nm. If operating in an environment in which the aerosol is strongly

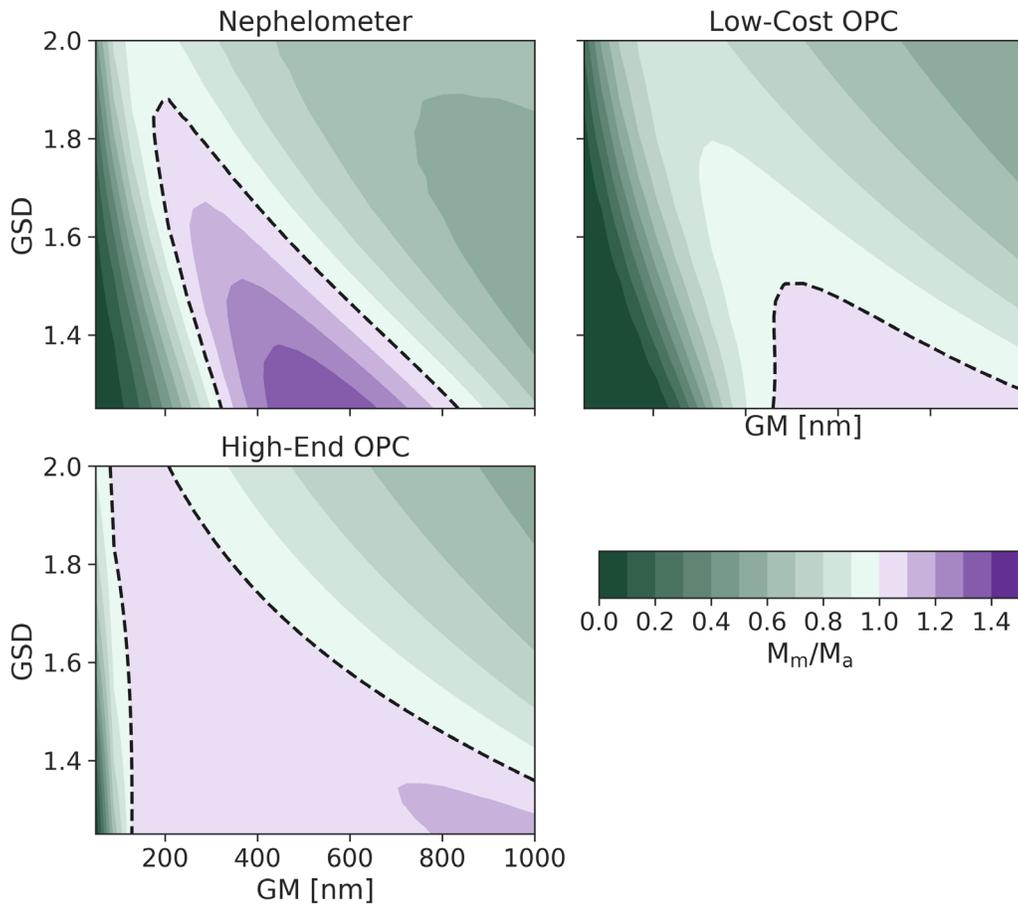
1 absorbing, large underestimates in  $PM_{2.5}$  should be expected. Even under conditions where the  
2 aerosol is not absorbing, the low-cost OPC largely underestimates the mass due to its high  
3 minimum size cutoff. For nephelometers, the errors are not as drastic, but still do depend  
4 strongly on the RI of the calibration aerosol used.

### 5 6 3.3 Changes in the Particle Size Distribution (PSD)

7 The ability of optical particle sensors to adapt to perturbations in the underlying particle size  
8 distribution (PSD) is important because PSDs can be highly variable over short periods of time,  
9 especially in urban areas with varying contributions from various local sources. Fig. 5 shows the  
10 accuracy of all three OPSs as the function of the PSD of the particles being measured. These  
11 calculations assume a single lognormal mode with all other properties of the aerosols (density,  
12 refractive index, and hygroscopicity) held constant. For the purpose of the model, the OPCs were  
13 calibrated using PSLs at each bin boundary, and the nephelometer was calibrated using  
14 ammonium sulfate ( $N=1e4 \text{ cm}^{-3}$ ,  $GM=400 \text{ nm}$ , and  $GSD=1.65$ ). The entire population of  
15 ammonium sulfate particles is then evaluated while varying the number-weighted mean particle  
16 diameter (GM) and the width of the distribution (GSD). For each PSD, we compute the relative  
17 accuracy of each device and plot the results in Fig. 5, in which the color and contours correspond  
18 to the  $M_m/M_a$  metric.

19  
20 The nephelometer substantially underestimates the mass concentration (by 50%-70%) for most  
21 PSDs, since it is calibrated to a single PSD. As the PSD changes, the ratio of total scattered light to  
22 integrated mass changes, causing the accuracy to change as well. (The accuracy depends  
23 somewhat on viewing angle, as shown in Figure S4, but errors are still substantial across a wide  
24 range of PSDs.) OPCs are potentially better since they measure the size of the particles and can  
25 theoretically account for changes in the PSD; however, they are still subject to errors given their  
26 limitations in detected size range. In particular, the low-cost OPC considerably underestimates  
27 the mass (by 60%-90%) for most PSDs as the bulk of the mass is below the detectable size limit  
28 of the OPC. As the geometric mean diameter increases in size, or the width of the distribution  
29 becomes larger, a larger fraction of the particles enters the detectable range, slightly improving

1 the results for the low-cost OPC. The high-end OPC is most able to adapt to the changes in the  
 2 PSD due to its significantly smaller  $D_{\min}$  (100 nm); there is roughly a 20% difference across the  
 3 entire range of PSDs shown. Unlike the low-cost OPC, a majority of the mass falls within the  
 4 detectable range of the high-end OPC, resulting in little to no effect of changes to the PSD on  
 5 accuracy of the mass concentration measurement.



6  
 7 **Figure 5.** Mass concentration accuracy ( $M_m/M_a$ ) of OPSs for a range of particle size distributions (PSDs).  
 8 Accuracy is shown for all combinations of PSDs with number-weighted geometric mean diameters (GMs)  
 9 between 100 - 1000 nm and geometric standard deviations (GSDs) between 1.2 – 2.0. Perturbations in  
 10 the PSD can lead to large errors for nephelometers and optical particle counters with high minimum  
 11 particle size cutoffs. All results are shown for ammonium sulfate particles; the OPCs were calibrated with  
 12 PSLs and the nephelometer was calibrated with ammonium sulfate ( $N=1e4 \text{ cm}^{-3}$ ,  $GM=400 \text{ nm}$ , and  
 13  $GSD=1.5$ ). A black dashed line indicates the “1:1” line, where  $M_m/M_a = 1$ .

14  
 15 While previous work has highlighted the importance of the varying PSD and its effect on making  
 16 accurate mass measurements with OPSs (Di Antonio et al., 2018; Gao et al., 2013; Malings et al.,

2020), the effect of ‘missing mass’ – the mass below the lowest size bin of an OPC – has received relatively little attention. The standard way to treat this missing mass is to empirically correct via regression analysis (Dacunto et al., 2015; Malings et al., 2020). While this can mitigate absolute errors, it requires the assumption that the PSD is constant in shape, varying only in magnitude. With particle loadings that are mostly below 10’s of  $\mu\text{g m}^{-3}$  throughout the United States, this assumption is unlikely to be a large source of absolute error. However, if the same approach were used in highly polluted environments where sub-300 nm aerosol loadings can easily reach hundreds of  $\mu\text{g m}^{-3}$  (Bhandari et al., 2020; Gani et al., 2019, 2020), changes in the PSD are likely to lead to large errors (in both an absolute and relative sense) in mass loading measurements. Overall, nephelometers and OPCs with high minimum size cutoffs are prone to substantial uncertainties as the underlying PSD changes, whereas for OPCs with low minimum size cutoffs this effect is relatively minor.

#### 4. Implications and future work

In this work, we have laid out a framework for understanding the sensitivity of low-cost optical particle sensors to the various physical and optical properties of aerosols. We described a new Mie theory-based software package (*opcsim*) for modeling the response of OPSs to various aerosols and demonstrated its use for better understanding the strengths and limitations of various low-cost particle sensors. We also used the model to investigate how various potential pitfalls (e.g., changes to environmental conditions, mismatches between calibration particles and particles being measured) may contribute to errors in mass concentration measurements. A summary of these results is given in Table 3.

**Table 3.** Effects of changing environmental/aerosol parameters on the relative error in measured mass loading by different OPS types.

Parameter changed	OPS type		
	Low-Cost OPC	High-End OPC	Nephelometer
RH & Hygroscopicity	Very high for (20-200%) for hygroscopic materials		

(Figure 2)	when RH > ~75%		
Optical Properties (Figure 4) <sup>1</sup>	High (30 – 100%)	Medium (20 – 60%)	Medium (20 – 75%)
Particle Size Distribution (Figure 5)	High 60 - 90%	Low < 20%	High 50 – 70%

1  
2  
3  
4  
5  
6  
7  
8  
9  
10  
11  
12  
13  
14  
15  
16  
17  
18  
19  
20  
21  
22  
23  
24  
25

<sup>1</sup> Primarily a source of error when an OPS calibrated with non-absorbing particles measures absorbing particles (or vice versa).

Consistent with previous studies, our results suggest that relative humidity is a large source of uncertainty for all **OPSS** when the aerosol is hygroscopic and relative humidities are above the deliquescence point, typically around 75%; additionally, the error introduced by relative humidity is highly sensitive to the aerosols’ affinity for water. This is correctable, at least to first order, limiting the impact of RH error on final results (Crilley et al., 2018; Di Antonio et al., 2018; Malings et al., 2020). Differences in aerosol optical properties can also lead to substantial errors in mass loadings for low-cost **OPCs**, with smaller but still substantial errors for high-end **OPCs** and nephelometers. This is especially important when the aerosol is strongly absorbing, as the amount of scattered light can make small particles undetectable with inexpensive optical detectors. If it were possible to measure some proxy for aerosol **composition in real time**, it would be possible to vastly reduce this error and improve the accuracy of mass measurements using **OPSS for real-time data collection**. **Additionally, this work highlights the importance of the underlying particle size distribution: differences in size distributions can lead to large errors in mass measurements from low-cost OPCs and nephelometers, while being only a small source of error for high-end OPCs that can properly count and size particles at low sizes. The ability of a given OPC to measure small particles is particularly important, with marginal improvements in minimum detected size leading to large gains in ability to accurately infer mass. Finally, the choice of calibrant is shown to be extremely important for both nephelometers and OPCs. Ensuring that OPSS are calibrated intelligently (i.e., using particles similar to the aerosol to be detected) can lead to significant improvements in expected performance.**

1 Table 4 summarizes these results within the context of measurements of representative real-  
2 world aerosol types. It provides an overview of the potential errors associated with different types  
3 of optical particle sensors under various scenarios, with recommendations for the type of calibration  
4 particles that would minimize errors in PM<sub>2.5</sub> mass measurements. Generally, in environments where  
5 small particles (< 300 nm) comprise a large percentage of the total mass, low-cost OPCs will be  
6 subject to considerable error. This will also be the case in environments with substantial levels of  
7 light-absorbing aerosol, such as wildfires or soot-heavy environments. (Sensor calibration using  
8 absorbing particles could help mitigate this effect, though this would introduce new errors when  
9 measuring non-absorbing aerosol.) In environments in which the underlying aerosol size distribution  
10 is variable (especially on short (sub-hour) timescales), such as urban environments or evolving  
11 wildfire plumes, nephelometers and low-cost OPCs will struggle to keep up with the changes in the  
12 relationship between the total scattered light and mass loading, leading to large variance in mass  
13 estimates.

14  
15 The estimates and recommendations given in Table 4 are not intended to be comprehensive, but  
16 rather serve as a starting point for characterizing the strengths and limitations of low-cost OPSs  
17 using Mie theory (and specifically the *opcsim* software package). Additional *opcsim* simulations  
18 carried out across a range of sensor designs, calibrant particles, and measured particle types  
19 could provide more comprehensive and quantitative estimates of errors in measured particle  
20 sizes and mass loadings, including for individual sensors and individual use-cases. Future  
21 improvements to *opcsim* could be made to allow for the simulation of more complex aerosols  
22 (e.g., externally-mixed populations, other particle morphologies) or the inclusion of more  
23 complex bin-assignment algorithms; comparison with laboratory studies (in which M<sub>m</sub>/M<sub>a</sub> is  
24 measured rather than just estimated) would also be useful. Additionally, co-located data with  
25 size-resolved measurements would allow for improved validation of the OPC component of this  
26 model. It is hoped that the Mie-theory-based approach described here will lead to an improved  
27 understanding of the errors associated with low-cost optical PM measurements, insight into  
28 calibration techniques that minimize such errors, and ultimately guidance into the design of new  
29 PM sensors for improved low-cost measurements of air quality and human exposure.

30  
31

**Table 4.** Summary of expected performance and recommendations for calibration materials for use of low-cost optical particle sensors to measure the particulate mass loadings of different aerosol types.

SENSOR PERFORMANCE BY OPS TYPE <sup>1</sup>					
AEROSOL TYPE	AEROSOL PROPERTIES	SUGGESTED CALIBRANT	Low-Cost OPC	High-End OPC	Nephelometer
FOSSIL-FUEL COMBUSTION	Very small GMD, mostly non-hygroscopic, moderate absorbing RI <sup>2</sup>	Calibrate with aerosols closer in RI, such as from combustion sources	Will perform poorly due to the small GMD and absorption component of the aerosol	Will perform moderately well though will miss ultrafine particles	Can perform moderately well if calibrated using appropriate materials
WILDFIRE	Varying PSD, moderate absorbing component of RI <sup>3</sup>	Calibrate with aerosol of similar optical properties and GMD (ideally biomass smoke)	Will likely undersize and underestimate mass due to the absorbing component of the aerosol; the GMD will change with proximity to the source leading to changes in accuracy	Will perform moderately well, though may mis-size the particles as the properties of the aerosol change as the plume evolves	Can perform well under certain circumstances; moderate error should be expected as the GMD of the wildfire plume evolves
URBAN	Varying GMD, moderate hygroscopicity <sup>4</sup>	Calibrate with NIST urban aerosol or collected urban aerosol	Performance depends on uniformity of sources; large errors will occur as aerosol source (and GMD) changes	Will perform moderately well to well, though will miss ultrafine particles	Will perform moderately well if averaged over a long period of time to normalize the GMD
DUST	Large GMD, non-hygroscopic <sup>5</sup>	Calibrate with Arizona Road dust or collected dust	Likely to perform well, given the large particle sizes	Likely to perform well, given the large particle sizes	Likely to perform well

<sup>1</sup> Based on properties of the aerosol only, and not external environmental parameters (i.e., RH).

<sup>2</sup> (Bond et al., 2002; Bond and Bergstrom, 2006; Chang et al., 2004)

<sup>3</sup> (Laing et al., 2016; McMeeking, 2004)

<sup>4</sup> (Hussein et al., 2004; Wehner and Wiedensohler, 2003)

<sup>5</sup> (Petzold et al., 2009; Rocha-Lima et al., 2018)

1 Acknowledgments

2 This work was funded by the Tata Center for Technology and Design at the Massachusetts  
3 Institute of Technology, as well as the US Environmental Protection  
4 Agency under assistance agreement RD-83618301. It has not been formally reviewed  
5 by the EPA; EPA does not endorse any products or commercial services mentioned in this  
6 publication. Additionally, the authors would like to thank Eben Cross and Timothy Onasch for  
7 helpful conversations regarding the operating principles of these sensors, Colette Heald for  
8 helpful suggestions regarding the summary of the paper, as well as the Kroll and Heald research  
9 groups at MIT for thoroughly testing the *opcsim* software package.

10

## 1 References

- 2 Abu-Rahmah, A., Arnott, W. P. and Moosmüller, H.: Integrating nephelometer with a low  
3 truncation angle and an extended calibration scheme, *Meas. Sci. Technol.*, 17(7), 1723–1732,  
4 doi:10.1088/0957-0233/17/7/010, 2006.
- 5 Ahlquist, N. C. and Charlson, R. J.: A new instrument for evaluating the visual quality of air, *J Air*  
6 *Pollut Control Assoc*, 17(7), 467–469, 1967.
- 7 Anderson, T. I., Covert, D. S., Marshall, S. F., Laucks, M. I., Charlson, R. J., Waggoner, A. P., Ogren,  
8 J. A., Caldow, R., Holm, R. I., Quant, F. R., Sem, G. J., Wiedensohler, A., Ahlquist, N. A. and Bates,  
9 T. S.: Performance Characteristics of a High-Sensitivity, Three-Wavelength, Total  
10 Scatter/Backscatter Nephelometer, *J. Atmos. Oceanic Technol.*, 13(5), 967–986,  
11 doi:10.1175/1520-0426(1996)013<0967:PCOAHS>2.0.CO;2, 1996.
- 12 Antonini, J. M., Lewis, A. B., Roberts, J. R. and Whaley, D. A.: Pulmonary effects of welding  
13 fumes: Review of worker and experimental animal studies, *American Journal of Industrial*  
14 *Medicine*, 43(4), 350–360, doi:10.1002/ajim.10194, 2003.
- 15 Apte, J. S., Brauer, M., Cohen, A. J., Ezzati, M. and Pope, C. A.: Ambient PM<sub>2.5</sub> Reduces Global  
16 and Regional Life Expectancy, *Environ. Sci. Technol. Lett.*, 5(9), 546–551,  
17 doi:10.1021/acs.estlett.8b00360, 2018.
- 18 Bhandari, S., Gani, S., Patel, K., Wang, D. S., Soni, P., Arub, Z., Habib, G., Apte, J. S. and  
19 Hildebrandt Ruiz, L.: Sources and atmospheric dynamics of organic aerosol in New Delhi, India:  
20 insights from receptor modeling, *Atmospheric Chemistry and Physics*, 20(2), 735–752,  
21 doi:https://doi.org/10.5194/acp-20-735-2020, 2020.
- 22 Bohren, C. F. and Huffman, D. R.: Absorption and scattering of light by small particles, John  
23 Wiley & Sons., 1983.
- 24 Bond, T. C. and Bergstrom, R. W.: Light Absorption by Carbonaceous Particles: An Investigative  
25 Review, *Aerosol Science and Technology*, 40(1), 27–67, doi:10.1080/02786820500421521,  
26 2006.
- 27 Bond, T. C., Covert, D. S., Kramlich, J. C., Larson, T. V. and Charlson, R. J.: Primary particle  
28 emissions from residential coal burning: Optical properties and size distributions, *Journal of*  
29 *Geophysical Research: Atmospheres*, 107(D21), ICC 9-1-ICC 9-14, doi:10.1029/2001JD000571,  
30 2002.
- 31 Bougiatioti, A., Bezantakos, S., Stavroulas, I., Kalivitis, N., Kokkalis, P., Biskos, G., Mihalopoulos,  
32 N., Papayannis, A. and Nenes, A.: Biomass-burning impact on CCN number, hygroscopicity and  
33 cloud formation during summertime in the eastern Mediterranean, *Atmospheric Chemistry and*  
34 *Physics*, 16(11), 7389–7409, doi:https://doi.org/10.5194/acp-16-7389-2016, 2016.

1 Burnett, R., Chen, H., Szyszkowicz, M., Fann, N., Hubbell, B., Pope, C. A., Apte, J. S., Brauer, M.,  
2 Cohen, A., Weichenthal, S., Coggins, J., Di, Q., Brunekreef, B., Frostad, J., Lim, S. S., Kan, H.,  
3 Walker, K. D., Thurston, G. D., Hayes, R. B., Lim, C. C., Turner, M. C., Jerrett, M., Krewski, D.,  
4 Gapstur, S. M., Diver, W. R., Ostro, B., Goldberg, D., Crouse, D. L., Martin, R. V., Peters, P.,  
5 Pinault, L., Tjepkema, M., Donkelaar, A. van, Villeneuve, P. J., Miller, A. B., Yin, P., Zhou, M.,  
6 Wang, L., Janssen, N. A. H., Marra, M., Atkinson, R. W., Tsang, H., Thach, T. Q., Cannon, J. B.,  
7 Allen, R. T., Hart, J. E., Laden, F., Cesaroni, G., Forastiere, F., Weinmayr, G., Jaensch, A., Nagel,  
8 G., Concin, H. and Spadaro, J. V.: Global estimates of mortality associated with long-term  
9 exposure to outdoor fine particulate matter, *PNAS*, 115(38), 9592–9597,  
10 doi:10.1073/pnas.1803222115, 2018.

11 Cerni, T. A.: Determination of the Size and Concentration of Cloud Drops with an FSSP, *J.*  
12 *Climate Appl. Meteor.*, 22(8), 1346–1355, doi:10.1175/1520-  
13 0450(1983)022<1346:DOTSAC>2.0.CO;2, 1983.

14 Chang, M.-C. O., Chow, J. C., Watson, J. G., Hopke, P. K., Yi, S.-M. and England, G. C.:  
15 Measurement of Ultrafine Particle Size Distributions from Coal-, Oil-, and Gas-Fired Stationary  
16 Combustion Sources, *Journal of the Air & Waste Management Association*, 54(12), 1494–1505,  
17 doi:10.1080/10473289.2004.10471010, 2004.

18 Chen, J., Li, Z., Lv, M., Wang, Y., Wang, W., Zhang, Y., Wang, H., Yan, X., Sun, Y. and Cribb, M.:  
19 Aerosol hygroscopic growth, contributing factors, and impact on haze events in a severely  
20 polluted region in northern China, *Atmospheric Chemistry and Physics*, 19(2), 1327–1342,  
21 doi:https://doi.org/10.5194/acp-19-1327-2019, 2019.

22 Cheung, H. C., Chou, C. C.-K., Lee, C. S. L., Kuo, W.-C. and Chang, S.-C.: Hygroscopic properties  
23 and CCN activity of atmospheric aerosols under the influences of Asian continental outflow and  
24 new particle formation at a coastal site in East Asia, *Atmospheric Chemistry and Physics*  
25 *Discussions*, 1–31, doi:https://doi.org/10.5194/acp-2019-519, 2019.

26 Chow, J. C. and Watson, J. G.: *Guideline on Speciated Particulate Monitoring.*, 1998.

27 Cohen, A. J., Brauer, M., Burnett, R., Anderson, H. R., Frostad, J., Estep, K., Balakrishnan, K.,  
28 Brunekreef, B., Dandona, L., Dandona, R., Feigin, V., Freedman, G., Hubbell, B., Jobling, A., Kan,  
29 H., Knibbs, L., Liu, Y., Martin, R., Morawska, L., Pope, C. A., Shin, H., Straif, K., Shaddick, G.,  
30 Thomas, M., van Dingenen, R., van Donkelaar, A., Vos, T., Murray, C. J. L. and Forouzanfar, M.  
31 H.: Estimates and 25-year trends of the global burden of disease attributable to ambient air  
32 pollution: an analysis of data from the Global Burden of Diseases Study 2015, *The Lancet*,  
33 389(10082), 1907–1918, doi:10.1016/S0140-6736(17)30505-6, 2017.

34 Crilley, L. R., Shaw, M., Pound, R., Kramer, L. J., Price, R., Young, S., Lewis, A. C. and Pope, F. D.:  
35 Evaluation of a low-cost optical particle counter (Alphasense OPC-N2) for ambient air  
36 monitoring, *Atmospheric Measurement Techniques*, 11(2), 709–720,  
37 doi:https://doi.org/10.5194/amt-11-709-2018, 2018.

1 Dacunto, P. J., Klepeis, N. E., Cheng, K.-C., Acevedo-Bolton, V., Jiang, R.-T., Repace, J. L., Ott, W.  
2 R. and Hildemann, L. M.: Determining PM<sub>2.5</sub> calibration curves for a low-cost particle monitor:  
3 common indoor residential aerosols, *Environ Sci Process Impacts*, 17(11), 1959–1966,  
4 doi:10.1039/c5em00365b, 2015.

5 Di Antonio, A., Popoola, O., Ouyang, B., Saffell, J., Jones, R., Di Antonio, A., Popoola, O. A. M.,  
6 Ouyang, B., Saffell, J. and Jones, R. L.: Developing a Relative Humidity Correction for Low-Cost  
7 Sensors Measuring Ambient Particulate Matter, *Sensors*, 18(9), 2790, doi:10.3390/s18092790,  
8 2018.

9 Dockery, D. W., Pope, C. A., Xu, X., Spengler, J. D., Ware, J. H., Fay, M. E., Ferris, B. G. and  
10 Speizer, F. E.: An Association between Air Pollution and Mortality in Six U.S. Cities, *New England*  
11 *Journal of Medicine*, 329(24), 1753–1759, doi:10.1056/NEJM199312093292401, 1993.

12 Gani, S., Bhandari, S., Seraj, S., Wang, D. S., Patel, K., Soni, P., Arub, Z., Habib, G., Hildebrandt  
13 Ruiz, L. and Apte, J. S.: Submicron aerosol composition in the world’s most polluted megacity:  
14 the Delhi Aerosol Supersite study, *Atmospheric Chemistry and Physics*, 19(10), 6843–6859,  
15 doi:https://doi.org/10.5194/acp-19-6843-2019, 2019.

16 Gani, S., Bhandari, S., Patel, K., Seraj, S., Soni, P., Arub, Z., Habib, G., Hildebrandt Ruiz, L. and  
17 Apte, J. S.: Particle number concentrations and size distribution in a polluted megacity: the  
18 Delhi Aerosol Supersite study, *Atmospheric Chemistry and Physics*, 20(14), 8533–8549,  
19 doi:https://doi.org/10.5194/acp-20-8533-2020, 2020.

20 Gao, R. S., Perring, A. E., Thornberry, T. D., Rollins, A. W., Schwarz, J. P., Ciciora, S. J. and Fahey,  
21 D. W.: A High-Sensitivity Low-Cost Optical Particle Counter Design, *Aerosol Science and*  
22 *Technology*, 47(2), 137–145, doi:10.1080/02786826.2012.733039, 2013.

23 Gucker, F. T., O’Konski, C. T., Pickard, H. B. and Pitts, J. N.: A Photoelectronic Counter for  
24 Colloidal Particles, *J. Am. Chem. Soc.*, 69(10), 2422–2431, doi:10.1021/ja01202a053, 1947.

25 Hagan, D. H. and Kroll, Jesse H.: dhagan/opcsim, Python. [online] Available from:  
26 <https://github.com/dhagan/opcsim> (Accessed 10 March 2020), 2019.

27 Hart, J., Eisen, E. and Laden, F.: Occupational diesel exhaust exposure as a risk factor for chronic  
28 obstructive pulmonary disease, *Current Opinion in Pulmonary Medicine*, 18(2), 151–154,  
29 doi:10.1097/MCP.0b013e32834f0eaa, 2012.

30 He, M., Kuerbanjiang, N. and Dhaniyala, S.: Performance characteristics of the low-cost  
31 Plantower PMS optical sensor, *Aerosol Science and Technology*, 54(2), 232–241,  
32 doi:10.1080/02786826.2019.1696015, 2020.

33 Henneberger, P. K. and Attfield, M. D.: Respiratory symptoms and spirometry in experienced  
34 coal miners: effects of both distant and recent coal mine dust exposures, *Am. J. Ind. Med.*,  
35 32(3), 268–274, doi:10.1002/(sici)1097-0274(199709)32:3<268::aid-ajim13>3.0.co;2-t, 1997.

- 1 Holstius, D. M., Pillarisetti, A., Smith, K. R. and Seto, E.: Field calibrations of a low-cost aerosol  
2 sensor at a regulatory monitoring site in California, *Atmospheric Measurement Techniques*,  
3 7(4), 1121–1131, doi:<https://doi.org/10.5194/amt-7-1121-2014>, 2014.
- 4 Hussein, T., Puustinen, A., Aalto, P. P., Mäkelä, J. M., Hämeri, K. and Kulmala, M.: Urban aerosol  
5 number size distributions, *Atmospheric Chemistry and Physics*, 4(2), 391–411,  
6 doi:<https://doi.org/10.5194/acp-4-391-2004>, 2004.
- 7 Jaenicke, R. and Hanusch, T.: Simulation of the Optical Particle Counter Forward Scattering  
8 Spectrometer Probe 100 (FSSP-100), *Aerosol Science and Technology*, 18(4), 309–322,  
9 doi:10.1080/02786829308959607, 1993.
- 10 Jurányi, Z., Tritscher, T., Gysel, M., Laborde, M., Gomes, L., Roberts, G., Baltensperger, U. and  
11 Weingartner, E.: Hygroscopic mixing state of urban aerosol derived from size-resolved cloud  
12 condensation nuclei measurements during the MEGAPOLI campaign in Paris, *Atmospheric  
13 Chemistry and Physics*, 13(13), 6431–6446, doi:<https://doi.org/10.5194/acp-13-6431-2013>,  
14 2013.
- 15 Koehler, K., Good, N., Wilson, A., Mölter, A., Moore, B. F., Carpenter, T., Peel, J. L. and Volckens,  
16 J.: The Fort Collins commuter study: Variability in personal exposure to air pollutants by  
17 microenvironment, *Indoor Air*, 29(2), 231–241, doi:10.1111/ina.12533, 2019.
- 18 Koehler, K. A., Kreidenweis, S. M., DeMott, P. J., Petters, M. D., Prenni, A. J. and Carrico, C. M.:  
19 Hygroscopicity and cloud droplet activation of mineral dust aerosol, *Geophysical Research  
20 Letters*, 36(8), doi:10.1029/2009GL037348, 2009.
- 21 Laing, J. R., Jaffe, D. A. and Hee, J. R.: Physical and optical properties of aged biomass burning  
22 aerosol from wildfires in Siberia and the Western USA at the Mt. Bachelor Observatory,  
23 *Atmospheric Chemistry and Physics*, 16(23), 15185–15197, doi:10.5194/acp-16-15185-2016,  
24 2016.
- 25 Levoni, C., Cervino, M., Guzzi, R. and Torricella, F.: Atmospheric aerosol optical properties: a  
26 database of radiative characteristics for different components and classes, *Appl. Opt.*, AO,  
27 36(30), 8031–8041, doi:10.1364/AO.36.008031, 1997.
- 28 Levy Zamora, M., Xiong, F., Gentner, D., Kerkez, B., Kohrman-Glaser, J. and Koehler, K.: Field  
29 and Laboratory Evaluations of the Low-Cost Plantower Particulate Matter Sensor, *Environ. Sci.  
30 Technol.*, 53(2), 838–849, doi:10.1021/acs.est.8b05174, 2019.
- 31 Lipsett, M. and Campleman, S.: Occupational exposure to diesel exhaust and lung cancer: a  
32 meta-analysis., *Am J Public Health*, 89(7), 1009–1017, doi:10.2105/AJPH.89.7.1009, 1999.
- 33 Malings, C., Tanzer, R., Hauriyluk, A., Saha, P. K., Robinson, A. L., Presto, A. A. and Subramanian,  
34 R.: Fine particle mass monitoring with low-cost sensors: Corrections and long-term  
35 performance evaluation, *Aerosol Science and Technology*, 54(2), 160–174,  
36 doi:10.1080/02786826.2019.1623863, 2020.

- 1 McMeeking, G. R.: Size Distribution Measurements of Wildfire Smoke-Influenced Aerosol at  
2 Yosemite National Park, 2004.
- 3 Northcross, A. L., Edwards, R. J., Johnson, M. A., Wang, Z.-M., Zhu, K., Allen, T. and Smith, K. R.:  
4 A low-cost particle counter as a realtime fine-particle mass monitor, *Environ Sci Process*  
5 *Impacts*, 15(2), 433–439, doi:10.1039/c2em30568b, 2013.
- 6 Osborne, S. R., Johnson, B. T., Haywood, J. M., Baran, A. J., Harrison, M. a. J. and McConnell, C.  
7 L.: Physical and optical properties of mineral dust aerosol during the Dust and Biomass-burning  
8 Experiment, *Journal of Geophysical Research: Atmospheres*, 113(D23),  
9 doi:10.1029/2007JD009551, 2008.
- 10 Patterson, H. S., Gray, R. W. and Sidgwick, N. V.: The scattering of light by the individual  
11 particles in smokes, *Proceedings of the Royal Society of London. Series A, Containing Papers of*  
12 *a Mathematical and Physical Character*, 113(764), 312–322, doi:10.1098/rspa.1926.0157, 1926.
- 13 Petters, M. D. and Kreidenweis, S. M.: A single parameter representation of hygroscopic growth  
14 and cloud condensation nucleus activity, *Atmospheric Chemistry and Physics*, 7(8), 1961–1971,  
15 doi:https://doi.org/10.5194/acp-7-1961-2007, 2007.
- 16 Petzold, A., Rasp, K., Weinzierl, B., Esselborn, M., Hamburger, T., Dörnbrack, A., Kandler, K.,  
17 Schütz, L., Knippertz, P., Fiebig, M. and Virkkula, A.: Saharan dust absorption and refractive  
18 index from aircraft-based observations during SAMUM 2006, *Tellus B*, 61(1), 118–130,  
19 doi:10.1111/j.1600-0889.2008.00383.x, 2009.
- 20 Pinnick, R. G., Garvey, D. M. and Duncan, L. D.: Calibration of Knollenberg FSSP Light-Scattering  
21 Counters for Measurement of Cloud Droplets, *J. Appl. Meteor.*, 20(9), 1049–1057,  
22 doi:10.1175/1520-0450(1981)020<1049:COKFLS>2.0.CO;2, 1981.
- 23 Raut, J.-C. and Chazette, P.: Retrieval of aerosol complex refractive index from a synergy  
24 between lidar, sunphotometer and in situ measurements during LISAIR experiment,  
25 *Atmospheric Chemistry and Physics*, 7(11), 2797–2815, doi:https://doi.org/10.5194/acp-7-  
26 2797-2007, 2007.
- 27 Rissler, J., Nordin, E. Z., Eriksson, A. C., Nilsson, P. T., Frosch, M., Sporre, M. K., Wierzbicka, A.,  
28 Svenningsson, B., Löndahl, J., Messing, M. E., Sjogren, S., Hemmingsen, J. G., Loft, S., Pagels, J.  
29 H. and Swietlicki, E.: Effective Density and Mixing State of Aerosol Particles in a Near-Traffic  
30 Urban Environment, *Environmental Science & Technology*, 48(11), 6300–6308,  
31 doi:10.1021/es5000353, 2014.
- 32 Rocha-Lima, A., Martins, J. V., Remer, L. A., Todd, M., Marsham, J. H., Engelstaedter, S., Ryder,  
33 C. L., Cavazos-Guerra, C., Artaxo, P., Colarco, P. and Washington, R.: A detailed characterization  
34 of the Saharan dust collected during the Fennec campaign in 2011: in situ ground-based and  
35 laboratory measurements, *Atmospheric Chemistry and Physics*, 18(2), 1023–1043,  
36 doi:10.5194/acp-18-1023-2018, 2018.

- 1 Seinfeld, J. H. and Pandis, S. N.: Atmospheric Chemistry and Physics: From Air Pollution to  
2 Climate Change, 2nd ed., John Wiley & Sons, New York., 2006.
- 3 Shepherd, R. H., King, M. D., Marks, A. A., Brough, N. and Ward, A. D.: Determination of the  
4 refractive index of insoluble organic extracts from atmospheric aerosol over the visible  
5 wavelength range using optical tweezers, *Atmospheric Chemistry and Physics*, 18(8), 5235–  
6 5252, doi:<https://doi.org/10.5194/acp-18-5235-2018>, 2018.
- 7 Sousan, S., Koehler, K., Hallett, L. and Peters, T. M.: Evaluation of the Alphasense Optical  
8 Particle Counter (OPC-N2) and the Grimm Portable Aerosol Spectrometer (PAS-1.108), *Aerosol  
9 Sci Technol*, 50(12), 1352–1365, doi:10.1080/02786826.2016.1232859, 2016a.
- 10 Sousan, S., Koehler, K., Thomas, G., Park, J. H., Hillman, M., Halterman, A. and Peters, T. M.:  
11 Inter-comparison of low-cost sensors for measuring the mass concentration of occupational  
12 aerosols, *Aerosol Science and Technology*, 50(5), 462–473,  
13 doi:10.1080/02786826.2016.1162901, 2016b.
- 14 Sumlin, B. J., Heinson, W. R. and Chakrabarty, R. K.: Retrieving the aerosol complex refractive  
15 index using PyMieScatt: A Mie computational package with visualization capabilities, *Journal of  
16 Quantitative Spectroscopy and Radiative Transfer*, 205, 127–134,  
17 doi:10.1016/j.jqsrt.2017.10.012, 2018.
- 18 Tryner, J., Quinn, C., C. Windom, B. and Volckens, J.: Design and evaluation of a portable PM 2.5  
19 monitor featuring a low-cost sensor in line with an active filter sampler, *Environmental Science:  
20 Processes & Impacts*, 21(8), 1403–1415, doi:10.1039/C9EM00234K, 2019a.
- 21 Tryner, J., Good, N., Wilson, A., Clark, M. L., Peel, J. L. and Volckens, J.: Variation in gravimetric  
22 correction factors for nephelometer-derived estimates of personal exposure to PM2.5,  
23 *Environmental Pollution*, 250, 251–261, doi:10.1016/j.envpol.2019.03.121, 2019b.
- 24 Ueda, S., Miura, K., Kawata, R., Furutani, H., Uematsu, M., Omori, Y. and Tanimoto, H.:  
25 Number–size distribution of aerosol particles and new particle formation events in tropical and  
26 subtropical Pacific Oceans, *Atmospheric Environment*, 142, 324–339,  
27 doi:10.1016/j.atmosenv.2016.07.055, 2016.
- 28 Walser, A., Sauer, D., Spanu, A., Gasteiger, J. and Weinzierl, B.: On the parametrization of  
29 optical particle counter response including instrument-induced broadening of size spectra and a  
30 self-consistent evaluation of calibration measurements, *Atmospheric Measurement  
31 Techniques*, 10(11), 4341–4361, doi:<https://doi.org/10.5194/amt-10-4341-2017>, 2017.
- 32 Wang, Y., Li, J., Jing, H., Zhang, Q., Jiang, J. and Biswas, P.: Laboratory Evaluation and Calibration  
33 of Three Low-Cost Particle Sensors for Particulate Matter Measurement, *Aerosol Science and  
34 Technology*, 49(11), 1063–1077, doi:10.1080/02786826.2015.1100710, 2015.
- 35 Wang, Z. B., Hu, M., Zeng, L. W., Xue, L., He, L. Y., Huang, X. F. and Zhu, T.: Measurements of  
36 particle number size distributions and optical properties in urban Shanghai during 2010 World

- 1 Expo: relation to air mass history, *Tellus B: Chemical and Physical Meteorology*, 66(1), 22319,  
2 doi:10.3402/tellusb.v66.22319, 2014.
- 3 Wehner, B. and Wiedensohler, A.: Long term measurements of submicrometer urban aerosols:  
4 statistical analysis for correlations with meteorological conditions and trace gases, *Atmospheric*  
5 *Chemistry and Physics*, 3(3), 867–879, doi:<https://doi.org/10.5194/acp-3-867-2003>, 2003.
- 6 Yin, Z., Ye, X., Jiang, S., Tao, Y., Shi, Y., Yang, X. and Chen, J.: Size-resolved effective density of  
7 urban aerosols in Shanghai, *Atmospheric Environment*, 100, 133–140,  
8 doi:10.1016/j.atmosenv.2014.10.055, 2015.
- 9 Zheng, T., Bergin, M. H., Johnson, K. K., Tripathi, S. N., Shirodkar, S., Landis, M. S., Sutaria, R. and  
10 Carlson, D. E.: Field evaluation of low-cost particulate matter sensors in high- and low-  
11 concentration environments, *Atmospheric Measurement Techniques*, 11(8), 4823–4846,  
12 doi:<https://doi.org/10.5194/amt-11-4823-2018>, 2018.
- 13 Zieger, P., Väisänen, O., Corbin, J. C., Partridge, D. G., Bastelberger, S., Mousavi-Fard, M., Rosati,  
14 B., Gysel, M., Krieger, U. K., Leck, C., Nenes, A., Riipinen, I., Virtanen, A. and Salter, M. E.:  
15 Revising the hygroscopicity of inorganic sea salt particles, *Nature Communications*, 8, 15883,  
16 doi:10.1038/ncomms15883, 2017.
- 17